Master Thesis

Model Predictive Control for Enhancing Wind Farms Participation in Ancillary Services

September 20, 2019

Author: Chloé Coral

Supervisor: Sara Siniscalchi Minna

Academic Supervisor: Eduardo Prieto Araujo

Acknowledgments

Here we are at the end of this journey. These past two years have been the most unpredictable years of my life, full of adventures, emotions, uncertainties, but most of all full of amazing people that I had the chance to have by my side. I want to share my gratefulness for all of them.

First of all I want to express my gratitude to my thesis supervisor Sara, for all she has done in this past six months. Thank you for your constant help and patience, and above all for becoming a friend.
Also, thank you Edu for your time, insights and support when I needed them.

Secondly, I want to thank my parents, Laurence and Giampietro, who gave me the possibility to be where I am, letting me choose my path and follow my passions without ever limit my decisions.

Furthermore, a huge thanks to my InnoEnergy family. Living abroad can be somehow destabilizing but it allows you to create bonds that are impossible otherwise. You all helped to create this magical adventure, that made me grow professionally but especially personally, and I will never be grateful enough for this. A special thanks to:
My flatmates, Fabio, Danilo, Hernan and Manu for making me feel at home.
Noran and Elsa, for being there.
The Osquldas gang, especially Zanzi and Cata, with who the Swedish winter never felt so warm.

Finally, thank you Max, for changing the way I see the world, and helping me to understand the kind of person I want to be.

Now, bringing with me all the memories and everything I have learned, it is time to continue to walk!

Abstract

The increasing penetration of Renewable Energy (RE) systems into the electric grid is creating new challenges into the power system. The unpredictable and variable nature of renewable power generation is increasing the imbalances between generation and demand. For this reason, wind farms, which are the main source of RE in Europe, are required nowadays to support the grid, providing services of voltage and frequency regulation.

To be able to increase their power production during a frequency event, Wind Power Plants (WPPs) need to work below their maximum generation capacity, keeping an additional amount of power, called power reserve, that can be injected into the grid when required.
The power reserve of a wind farm strongly depends on the interaction among the wind turbines. The wake effect produced by the upstreams turbines affects the wind condition that each turbine faces and reduces their maximum available power.

This study aims to present the effects of different distribution of the Wind turbines (WTs) individual power contribution on the power reserve. Three control strategies, based on Model Predictive Control (MPC), are tested on a fifteen turbines wind farm under different wind conditions. Simulation results show that, in almost all cases, prioritizing the power contribution of the most downstream turbines and deloading the upstream ones, leads to a maximization of the wind farm power reserve.

Furthermore, an additional MPC strategy aiming to combine active and reactive power control, for providing both frequency and voltage regulation at the Point of Common Coupling (PCC), is presented. The advantage of a combined active and reactive power control is the possibility of improve the voltage support capability of the WPPs, by controlling the active power set-points. The MPC is also tested on a fifteen turbines wind farm, in order to validate the performances of the controller while solving the multi-objective problem. The ability of the controller to handle simultaneously the different requirements is proven.

Contents

List of Figures

List of Tables

Acronyms

AIC Axial Induction Control. 24

APC Active Power Control. 22, 24, 25, 27, 28

CFD Computational Fluid Dynamics. 23

DFIG doubly fed induction generator. 19

GHG Green house gases. 13

HAWT Horizontal axis wind turbine. 16

KE Kinetic Energy. 28

MPC Model Predictive Control. 4, 6, 15, 25, 29, 32, 34–36, 43, 49, 50, 59

PCC Point of Common Coupling. 4, 15, 49, 50, 52, 53, 59, 60

PMSG permanent magnet synchronous generator. 20

PV Photovoltaic. 13

RE Renewable Energy. 4, 14, 15

SCIG Squirrel cage induction generator. 7, 18, 19

TSOs Transmission System Operators. 14, 26, 29, 45, 50, 59

VAWT Vertical axis wind turbine. 16

WPPs Wind Power Plants. 4, 59, 61

WRC Wake Redirection Control. 24

WRIG wound rotor induction generator. 19

WRSG wound rotor synchronous generator. 20

WTs Wind turbines. 4, 17, 34, 40, 43, 45, 60

Chapter 1

Introduction

1.1 Motivation

The global energy demand, due to the expected rising incomes and population growth, is assumed to raise by more than a quarter by 2040, and the Green house gases (GHG) emissions from the energy sector, nowadays accounting for 32.5 Gt per year, are expected to raise till 35.88 Gt. The largest contribution to GHG is, by far, coal-fired power generation, with a 27% of the total emissions [1]. Therefore, it is clear that in order to fight climate change and achieve the COP21 temperature goal, a transition and de-carbonisation of the energy sector is necessary.

Since the early 2000s the expansion of renewable technologies has been exponential, especially for wind and solar PV. The renewable capacity installed worldwide passed from 800 GW in 2004 to 2351 GW in 2018 according to the data in [2] and [3], and is expected to reach a share in power generation of over 40% by 2040 [1].

Wind power especially, is having a significant role in achieving the climate change and energy commitments in the power sector. In Europe, wind energy has experienced an exponential growth in the past ten years, Figure 1.2, becoming the second energy source for installed capacity, only below natural gas. With an installed capacity of 182 GW [3], wind power generation was able to meet the 14% of the EU electricity demand in 2018 [4].
This trend is expecting to growth even more in the next decade. According to the WindEurope's central scenario the total installed capacity should reach 323 GW in 2030, with the potential to meet 29.6% of Europe's electricity demand [5].

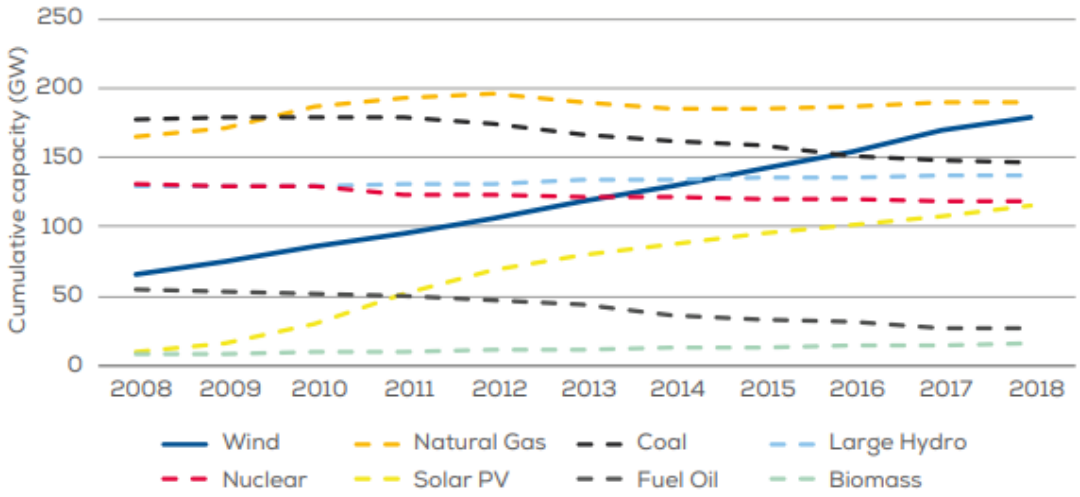

Figure 1.1: Total power generation capacity in the European Union 2008-2018 [4]

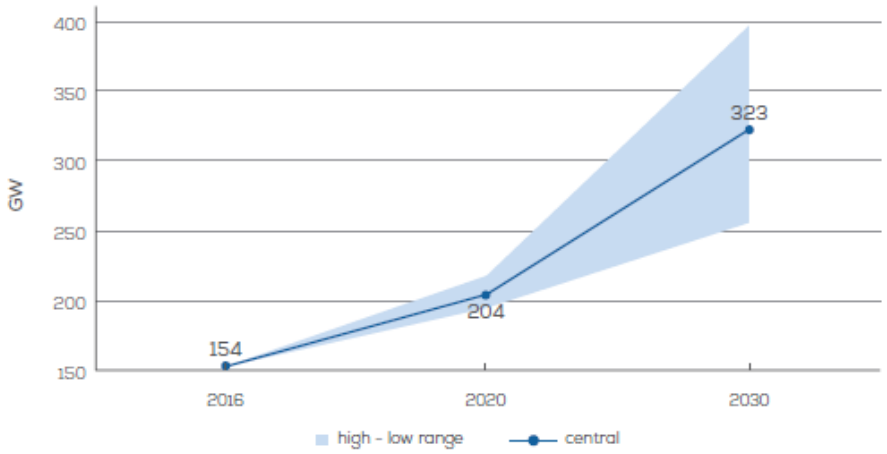

Figure 1.2: WindEurope 2020 and 2030 scenario [5]

However, the fast expansion of the renewable energy market is creating new challenges in the energy sector. The variable, unpredictable and decentralised nature of renewable resources, especially wind and solar, requires a new kind of flexibility in the power system. The increase of RE installations, along with the decrease of conventional synchronous generation, leads to an increase of the imbalances between generation an demand and an increasing need of grid regulation services. Large wind farm are now also required from Transmission System Operators (TSOs) to take part in ancillary services and contribute to frequency regulation by injecting additional power into the grid [6].

The purpose of the following work is to propose a novel control strategy aiming to improve the participation of wind farms in ancillary services, focusing especially on frequency sup-

port. Improving wind farms performances in frequency regulation will lead to solve some of the issues of RE grid integration, along with a reduction of the cost of wind energy and therefore boost the deployment of wind power generation.

1.2 Objectives

The main goal of this study is to design a wind farm control strategy, based on Model Predictive Control (MPC), that maximizes the primary reserve of the wind farm, while generating the amount of power required by the grid operator. By maximizing the primary reserve, the additional capacity available for grid frequency regulation is increased.

In a wind farm, the wake effect produced by the wind turbines affects the performance of the plant, and it is strictly dependent on the power generated by each turbine. Therefore, three different control strategies, aiming to distribute the individual power contribution of each wind turbine with different configuration, are formulated. The distribution considered are the proportional one, with individual power set-points proportional to the available power, the equal distribution, where the power demand is equally split among all the turbines and the backward distribution, which aims to prioritize the generation of the downstream turbines. Hence, to find the best control approach for the maximization of the power reserve, the three control strategies are compared under different scenarios of wind conditions and power demand.

Furthermore, as grid codes also require wind farms to provide voltage regulation support, a control strategy that takes into account voltage regulation at the PCC, while meeting the precedent requirements of power reserve maximization and tracking of the power demand, is also presented.

The work is organised as follows: in Chapter 2 an overview of wind power generation and the challenges that it entails, such as wind farm control and integration into the power system, are presented. Chapter 3 describes the control problem and the proposed MPC strategies. In Chapter 4 the simulations results of the three control strategies are compared. In Chapter 5 a further control strategy, which considers reactive power control for voltage support, is formulated and validated. Finally, conclusions are drawn in Chapter 6.

Chapter 2

Wind power generation

2.1 Wind turbine fundamentals

Wind has been exploited as an energy source since early ages, such as windmills used for wheat grinding and irrigation. However, the first developments of electric power generation through wind turbines started in the 70s of the nineteenth century. Different designs of wind turbines have been proposed through the years, such as vertical axis (VAWT) like Savonius, Darrieus or Giromill rotor, or horizontal axis turbines(HAWT) as the most common commercialized three-bladed rotor [7]. The technological development of the wind turbines in the last decades has been significant: while at the end of the century the existent wind turbines had a capacity of slightly more than 1 MW, the improvements made in the dimensions of the rotor diameter have lead to the construction and deployment of more powerful turbines, reaching also 10 MW of capacity, Figure 2.1.

A typical structure of a horizontal axis wind turbine is presented in Figure 2.2. The rotor is

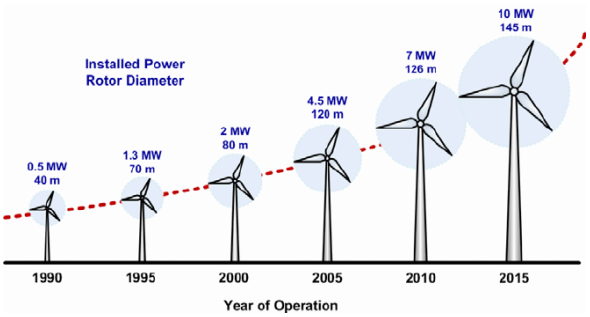

Figure 2.1: Size evolution of wind turbines over time [8]

composed by the blades, the hub and the shaft. The energy from the wind is collected by the blades and transferred to the generator through the mechanical shaft. Generally, a gearbox is present in order to adapt the speed of the rotor blades to the higher speed of the generator. In some types of wind turbines, regulated by power electronics, the gearbox is not necessary. These different types of wind turbine generators, mainly induction or synchronous machines, will be presented in Section 2.1.1. Both generator and gearbox are placed in the nacelle. After the conversion from mechanical to electric power operated by the generator, a transformer, conventionally situated in the tower, adapts the wind turbine voltage to the one of the collector bus of the wind farm [9]. To regulate the mechanical power delivered by the rotor the control variables are tipically:

- Blade pitch (θ) - The angle of the blades is controlled, using hydraulic actuators or servo pitch motors, in order to influence the power capture and maintain the machine under its power limits.
- Generator Torque (τ_g) - The torque of the generator is used to control the power extraction.
- Yaw (γ) - The yaw system controls the rotation of the nacelle, generally aiming to have a yaw angle γ equal to zero, which means that the rotor is perpendicular to the wind direction. The yaw angle can be controlled also for wake redirection (Section 2.2.2).

While the elements presented till now are the same for both offshore and onshore wind turbines, the foundation of the WTs differs in the two cases: for the latter the turbines are installed on a concrete base while for offshore WTs the foundation structure can be either attached to the sea bed either a floating one [9].

2.1.1 Types of Wind Turbines

As mentioned previously, from the electrical point of view different types of wind turbines have been proposed through the years and can be classified as following [10]:

- Fixed-speed wind turbine
- Limited variable-speed wind turbine
- Variable speed with partial-scale converter

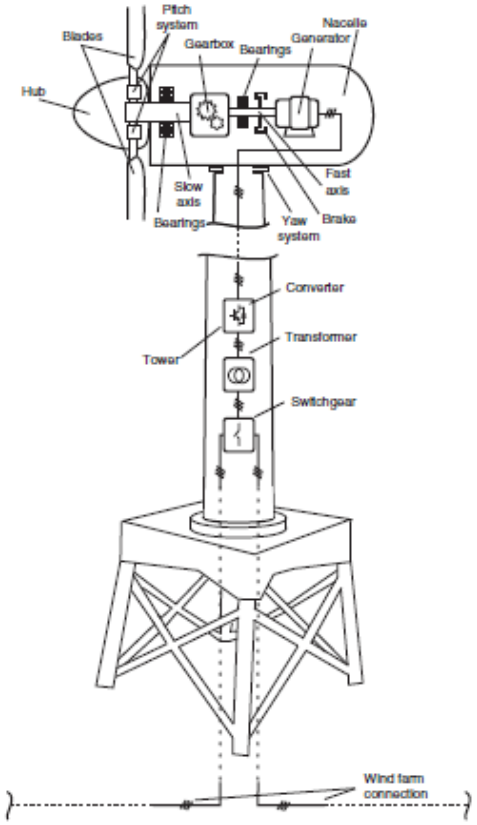

Figure 2.2: HAWT scheme [9]

- Variable speed with full-scale converter

Fixed-speed Wind Turbine

At the beginning of the commercialization of the wind turbines, the most common type installed was the fixed speed one. This solution was made of a three bladed rotor, a multistage gearbox, a soft-starter for a smoother grid connection, a capacitor bank for reactive power compensation and a squirrel cage induction generator (SCIG) directly connected to the grid through a transformer. This type of turbine has the advantage of being simple, robust and reliable. The main drawback is that the direct connection to the grid obliges the generator to rotate at a synchronous speed and does not optimize the extraction of the available power from the wind. Further problems are the impossibility of providing voltage/frequency support and the fault ride-through capability: as directly connected to the grid, it is difficult to avoid a disconnection in case of high currents due to a fault in the network [9].

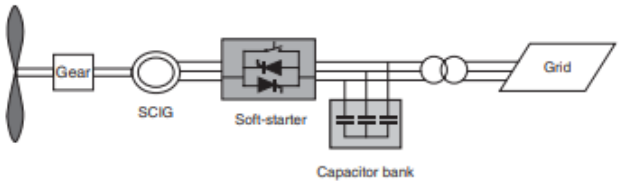

Figure 2.3: Fixed-speed wind turbine with SCIG [10]

Limited Variable-speed Wind Turbine

The idea behind a variable speed system is to keep the generator torque constant while the wind variations are absorbed by changes in the generator speed. To increase the aerodynamic efficiency of the turbine, in the 1990s, Vestas proposed a new type of turbine, with a wound rotor induction generator (WRIG) and introducing a variable rotor resistance. The value of the rotor resistances can be changed through a power converter producing a variation of the machine slip and consequently of the generator speed. Typically, the speed operation range is from 0% to 10% above the synchronous speed [10]. The need of having a variable speed was partially solved with this configuration but the problems of the fixed-speed concept were not completely solved.

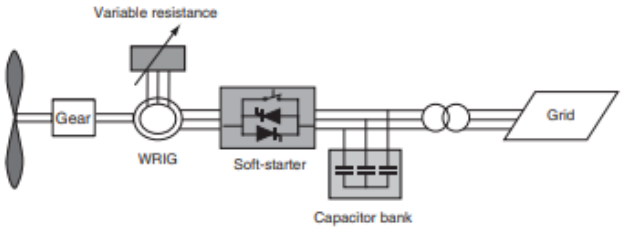

Figure 2.4: Limited variable-speed wind turbine with WRIG and variable resistance [10]

Variable speed with Partial-scale Converter

This type of turbine, known as doubly fed induction generator (DFIG), consists of a WRIG generator connected to the grid directly by the stator and through the rotor by a partial-scale power converter. The converter is able to wider the speed range, going from -40% to +30% of the synchronous speed. Furthermore the converter is able to do a proper active and reactive power control, and a better ride-through capability is achieved [9]. The smaller size of the converter (rated around 30% of the nominal generator power) makes this concept attractive

from an economical point of view. Still some drawbacks are present as the use of slip rings and protection in the case of grid faults, as the stator is still directly connected to the grid.

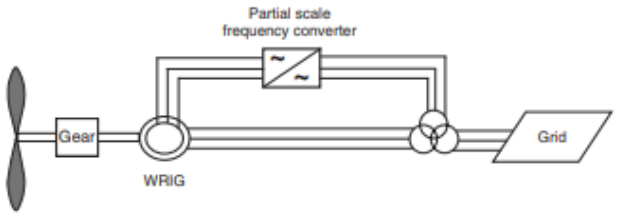

Figure 2.5: DFIG Wind Turbine [10]

Variable speed with Full-scale Converter Wind Turbines

The variable speed with full-scale converter concept maximizes the speed range of the machine and allows the maximum power extraction from the wind within the rated limits. This system can give voltage and frequency support to the grid and can incorporate ride-through strategies. Also, the gearbox is not necessary anymore. The solution can be implemented for different types of generator: SCIG, permanent magnet synchronous generator (PMSG), and wound rotor synchronous generator (WRSG) [9].

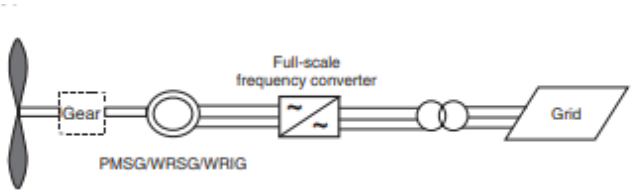

Figure 2.6: Variable speed with Full-scale Converter Wind Turbine [10]

Nowadays in wind industry, the most employed turbine is the type 3, due to its good performance in different wind conditions, the possibility of grid support and its relatively low cost (due to the smaller size of the converter) if compared to type 4. However, as converters are becoming cheaper and their capacity is increasing, the full-scale converter type is receiving more attention from the market. Especially for off-shore wind farms, where maintenance is more costly and complicated, the use of type 4 WT is being preferred as the rate of failure, due also to the non-presence of the gearbox, is lower [11].

2.1.2 Power production characteristics

The power of an air mass that flows at speed V through an area A represents the total available energy per unit of time and can be calculated as follows:

$$P_{wind} = \frac{1}{2}\rho A V^3 \text{ [W]} \tag{2.1}$$

where:

ρ = air density (kg/m^3);

V = wind speed (m/s).

When the power in the wind is converted into the mechanical energy of the wind turbine rotor the results is a lower speed of the air mass. As the air mass can not be stopped completely after flowing through the rotor area, the power available in the wind can not be totally extracted. The theoretical optimum for utilising the power in the wind by reducing its velocity was discovered by Betz in 1926 and corresponds to 59% of the total available power [12]:

$$P_{Betz} = \frac{1}{2}\rho A v^3 C_{p,Betz} = \frac{1}{2}\rho A v^3 \times 0.59 \tag{2.2}$$

While the $C_{p\ Betz}$ is the theoretical limit, the power coefficient (C_p) of a wind turbine is the parameter that represents the aerodynamic efficiency of the rotor (for modern wind turbines in the range of 0.4-0.5 [13]). The C_p is generally a function of the tip speed ratio for low wind speed (region 1, Figure 2.8), and a function of the pitch angle for wind speed higher than the rated speed (region 2, Figure 2.8). The tip speed ratio λ is defined as follows:

$$\lambda = \frac{\Omega R}{U} \tag{2.3}$$

where Ω is the angular velocity of the rotor, R the rotor radius and U the incident wind speed. A typical curve of the relationship between C_p and λ is shown in Figure 2.7. It can be noticed that in order to maximize the power coefficient, the tip speed ratio has to be held constant, which means that the rotor speed need to be controlled according with the wind speed. This is the reason why a variable-speed turbine has better aerodynamic performances than fixed-speed ones.

Figure 2.8 shows the power curve of a wind turbine. In region 1 the machine starts generating power at a certain wind speed (cut-in wind speed) and, as presented in (2.2), the power generated increases with the increasing wind speed till the rated one, at which the turbine is designed to produce its rated power. At wind speeds higher than the rated wind speed,

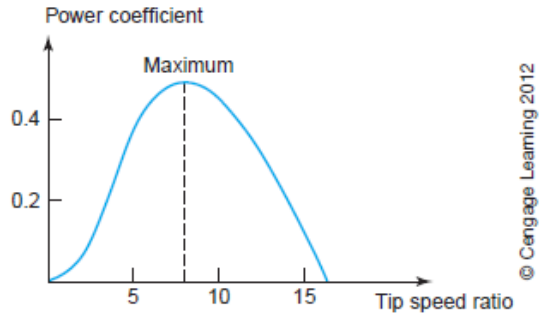

Figure 2.7: Typical $C_p - \lambda$ curve for a wind turbine [7]

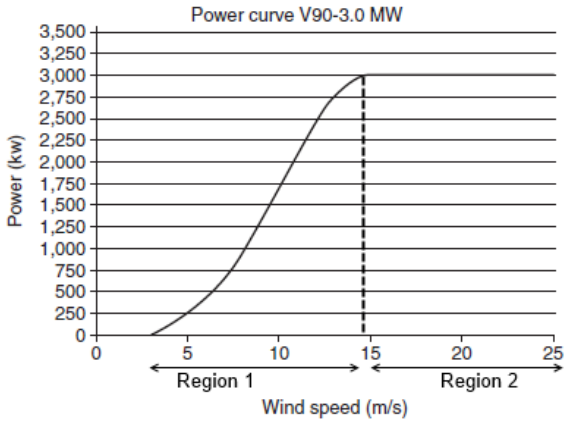

Figure 2.8: Power curve for the Vestas V90, 3.0 MW turbine [13]

region 2, the wind turbine keeps producing its rated power till the cut-out wind speed, at which the turbine is shut down to avoid structural damages, for instance during a storm.

2.2 Wind farm control

Wind turbines are usually grouped in wind farms, as it reduces the deployment costs of the turbines and the electricity grid, operation and maintenance costs and the land use and impact. However, the wake produced by every turbine reduces the wind speed and increases turbulence, affecting the other downstream turbines. This leads to a reduced energy extraction and to higher mechanical loads on each of them, which reduce the lifetime of the turbines. These effects increase the overall cost of wind energy [14].

Therefore, the goal of wind farm control is to minimize the cost of wind energy, through different technical objectives such as the maximization of the power production, the minimization of the structural degradation and active power control (APC) for grid support.

While the typical control strategies used were aiming to maximize the output of each wind turbine individually, the new control approaches take into consideration the interaction between the turbines in order to increase the performances of the wind power plant and reach the previously mentioned objectives . To be able to account these interactions while building the control strategy, the whole system needs to be properly modelled. Due to the complexity of this task, several already implemented and on-going researches have been focusing on the wind flow field and wake effects in order to optimize the wind farm power generation.

2.2.1 Wind farm modeling

Modern control algorithms rely on internal models which are considered low fidelity (or parametric) models. These kind of models are often simple and not computationally expensive and therefore suitable for real-time control. On the other hand, high fidelity models, which are more accurate but also significantly more computationally expensive, are generally used to asses controller performances. Two main components can be identified in wind farm models: the turbine model, used to predict the dynamics of the wind turbine power response, and the flow model, which predicts the aerodynamics interactions among the turbines due to the wake effects [14]. Typically, non-linear systems governed by the three dimensional Navier-Stokes equations should be used to properly describe the highly variable nature of the wind flow field through a wind farm. However, no analytic solutions has been found yet for these equations and computational fluid dynamics (CFD) uses numerical analysis and algorithms to solve this problem. However, due to the computational weight of these solutions, two dimensional and parametric models that only estimate specific characteristics of a wake, such as wake deflection and speed velocity, have also been developed. An example is the Jensen Park model, which predict the linear expansion of the wake and the velocity deficit, only depending on the distance behind the rotor [15]. The interested reader can find an extensive overview of the different wake models adopted for wind farm modeling in [14].

2.2.2 Wake control

Nowadays, most of the wind farms are operated using individual wind turbine control setting that consist in finding the optimal power set point for each wind turbine. The control

of a wind farm relies instead on the assumption that, the operation of the turbines away from their optimal settings can lead to an increase of the wind farm performances. For this purpose two main methods are used: *axial induction control* (AIC) and *wake redirection control* (WRC) [14]. The former is based on the idea that, reducing the power output of the upstream wind turbines, by controlling the axial induction, the downstream ones can increase their production. The method is worth it in case of significant wake effect and if downstream wind turbines performances are highly affected by it. However, as presented in [14], although the research in the field is being widely developed, there are no clear results on the feasibility of this approach for the maximization of the power extraction. Results strongly depend on the models used, as for steady-state parametric models several studies illustrate that AIC increases the power output of the wind farm, while high fidelity studies show that this is not always possible. Nevertheless, in other works, AIC has been used to decrease structural loads and for Active Power Control (see Section 2.3.4).
In WRC approach the upstream turbine's rotor is misaligned with the incoming flow in order to produce a deflection of the wake that will not or just partially overlap the downstream turbine. This can be done by pitch control, tilt or yaw actuation. Several studies show that, in simulations, wake redirection promises significant improvements in power production output [14].

2.2.3 Wind farm control strategies

For controlling wind farms, due to the uncertainty and time-varying wind flow conditions, it is necessary to use a feedback control approach that can react fast to the changes of wake and wind flow direction and speed. Wind farm controllers can be centralized or non-centralized [16], however, for the purpose of this work only centralized controller will be considered. In this approach, a central power plant controller determines, according to the desired strategy, the individual control settings of each turbine and forwards them to the single turbine controllers. Then, these internal controllers ensure the tracking of the set point received, modifying the blade pitch and generator torque (Section 2.1).
Closed-loop approaches employ internal models and measurements, which can be atmospheric conditions and values of power production. With these values as a feedback, the control actions can adapt to the change of properties and the individual power set point of the turbines can be modified dynamically (Figure 2.9). As it is extremely hard to measure all the states of the model and feed them to the controller, in closed-loop output feedback

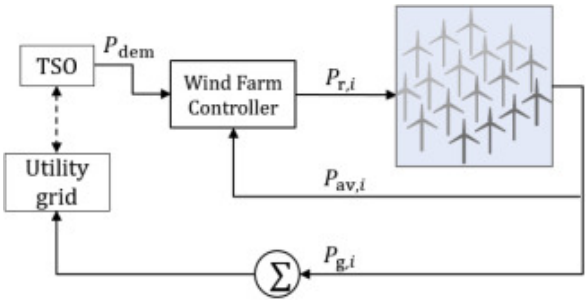

Figure 2.9: General wind farm control system [17]

only a sub-set of states is measured and the control action evaluated on its base. In addition, observers can be used to estimate all the states of the system through few measurements [14].

Several studies have been conducted in order to control the wake effect and increase performances with closed-loop control strategies. In [18] it is shown how using a feedback control can improve the power tracking performance of a wind farm, in case of high wake effect, compared to an open-loop approach as the one used in [19]. In [20], authors develop an adjoint-based model predictive controller that employs a medium-fidelity 2D model, with the aim of minimize power losses under time-varying changes of the atmospheric conditions. In [14] different closed-loop control strategies for power extraction optimization, based on game theory, extremum seeking control and Model Predictive Control are presented and compared.

As the purpose of this work is to build a control strategy for APC, approaches regarding active power control on wind farm will be further analysed in Section 2.3.4.

2.3 Integration of wind power into the power system

2.3.1 Power balance

For normal operation of the power system, frequency and voltage need to be stable. Conventionally, frequency is regulated by controlling active power while voltage by reactive power. For this reason, the principal function of the power system is to always meet the energy demand and have a constant balance between generation and consumption. Changes in power supply or demand lead to a temporary imbalance of the system and affect operating conditions of power plants as well as consumers. In European countries, the frequency usually

lies between 50 ± 0.15 Hz [21]. Large drops in frequency can trigger a cascade tripping of power stations and lead to a complete shutdown of electricity supply or blackout, which full restoration may take several days. It is important therefore to maintain the frequency controlled.

Frequency is directly connected to the rotational speed of the generators. For the energy conservation law, at any instant the power demanded by the load needs to be supplied by the generators and/or by energy stored within the system. In synchronous generators, if the load is suddenly increased, the extra energy is firstly supplied by the rotational inertia of the generator through a decrease of its speed. This decrease in speed leads to a proportionate decrease in frequency. In conventional generation, as connected to the grid, in case of frequency events the governor is in charge of automatically adjusting the fuel supplied in order to stop the frequency drop and reach a new equilibrium.

2.3.2 Power reserves

The maintenance of the frequency involves additional active power that can be delivered from a generating unit after an event occurs. According with different timescales, four power reserve levels can be defined: inertia, primary, secondary and tertiary reserve (Figure 2.10) [22].

- **Inertia response**: follows immediately the frequency event, the synchronous generators start decelerating and provides kinetic energy that was stored in their rotating mass.

- **Primary reserve**: within a timescale of second/minutes is intended to be the additional capacity of the network that can be automatically and locally activated by the generator's governor after a few seconds at most of an imbalance of electricity in the network. The aim of primary reserve is to stop the frequency fall and stabilize it to a new equilibrium value.

- **Secondary reserves**: with a duration that can reach a few hours, they are activated for restoring the rated frequency of the system, to release primary reserves and to restore active power interchanges between control areas to their setpoints. They can be activated either automatically or through the change of active power setpoints made by the TSOs.

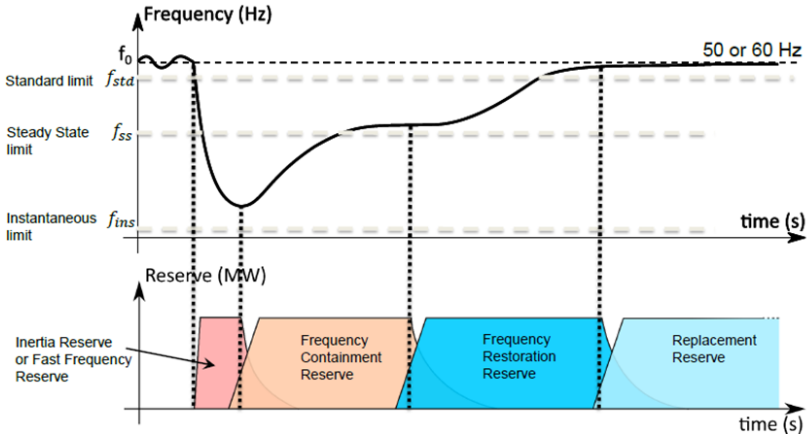

Figure 2.10: Deployment of power reserves [23]

- **Tertiary reserves**: actuating for several hours, they replace the secondary reserves, to manage eventual constraints in transmission lines, and to bring back the frequency to its rated value if secondary reserves are not sufficient. These reserves are activated manually and centrally at TSO control centres, in case of observed sustained activation of secondary reserves.

2.3.3 Wind turbines and ancillary services

The increase of renewable generation into the power system is leading to a decrease of conventional generation that is crucial for ancillary services, as they play a fundamental role in grid stabilization. Especially at levels of high participation of wind energy in the electricity mix and in isolated grids, renewable power plants are now also required to provide support to the grid. In [6], different examples of grid codes established by TSOs referring to the participation of wind power in frequency regulation are illustrated.

As modern wind turbines (type 3 and 4) are decoupled from the grid frequency through power electronics (Section 2.1.1), and the turbines do not participate automatically in frequency regulation response, to do so, wind farms need to be controlled through Active Power Control, which aims to control the active power output of a wind farm in order to assist the balance between generation and demand.

Some studies also show the economical potential benefits for wind power plants operators to participate in the ancillary services market [24]. As the purpose of this work is to define a control strategy for primary frequency support, a review of the current state of art for APC on wind farms will be presented in the next section.

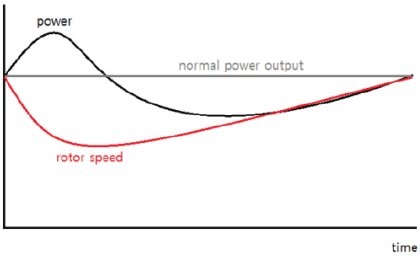

Figure 2.11: Inertial response emulation for a frequency droop [6]

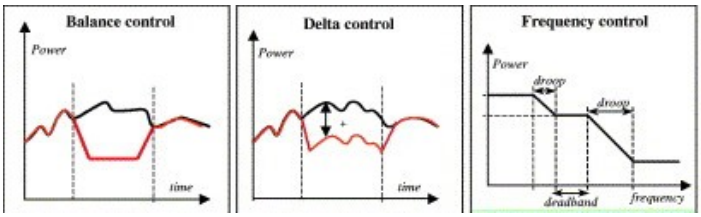

Figure 2.12: Wind farm control functions [25]

2.3.4 APC on wind farms

APC on wind turbines is being used for two different purpose. The first is to emulate the inertial response of conventional generators immediately after a frequency event, providing Kinetic Energy (KE), through the deceleration of the wind turbine rotor (Figure 2.11) This generally performed by controlling the generator torque. However, after the frequency event, to restore the optimal operational set point new KE need to be provided from the grid. The other application of APC is to track, over longer time scales, a power reference from the TSOs as a secondary response. This implies to operate permanently in sub-optimal conditions (de-loading operation mode). The function that can be required by the TSO are (Figure 2.12):

- Balance control: constant reduction of active power.
- Delta control: proportional reduction based on the amount of renewable generation. The aim is to have at all time an available power reserve that can be used for frequency regulation.
- Ramp rate control: sets how fast the production can be adjusted upwards or downwards.

In both cases, there is a growing interest in increasing performance of APC on wind farms, and several studies have been carried out with the objective of improving the frequency

support capability of the wind power plants. In [26] a control strategy aiming to maximise the total KE of the wind farm, taking into account wake interaction among WTs, was proposed. The results show that, deloading the upstream WTs and controlling the rate of KE injected into the grid during a frequency event, it was possible to keep the system frequency relatively uniform and provide a valuable primary frequency control service. In [25], in the context of secondary response, a central controller able to meet different multiple control tasks imposed by the TSOs, such as delta and balance control, is illustrated. The authors in [27] show a model-based receding horizon control, that is able to provide up-regulation with deratings lower than the maximum up-regulation requested, by leveraging the aerodynamics effect among the wind turbines. The study in [28] illustrate a maximization of the power reserve through a MPC strategy that uses a lexicographic optimization that takes into consideration the wake effect. The strategy aims to distribute the power contribution of each turbine to obtain the total demanded power and maximize the total power reserve. The same authors, in [16], propose a controller that prioritize the power contribution of the most downstream turbines in order to reduce the wake effect and increase the power reserve, still tracking the power set point set by the system operator. Results show that, compared with the conventional power distribution where the set-point of each turbine are proportional to the available power, there is an augment in power reserve that can be used for frequency regulation. Other previous studies regarding primary and secondary response are presented in [6].

Chapter 3

Optimization problem

3.1 Wind turbine model

In the context of high wind power participation in the electricity mix wind farms are usually operated in de-loading mode, which means that the power generated is kept below the total available power, in order to have an amount of power, known as power reserve, that can be used for grid frequency support. The power reserve is the quantity that the proposed optimization problem will aim to maximize.

The power reserve of a wind farm can be defined as the sum of the power reserves of each wind turbine and it is represented by the difference between available and generated power:

$$P_{res,tot} = \sum_{i=1}^{n_t} P_{res,i} = \sum_{i=1}^{n_t} \left(P_{av,i} - P_{g,i}\right) \tag{3.1}$$

The generated power by the i-th wind turbine depend on the tip speed ratio λ and pitch angle β and is defined as:

$$P_{g,i} = \frac{1}{2}\rho A v_i^3 C_p(\lambda_i, \beta_i) \tag{3.2}$$

while the available power is the minimum between the maximum power extractable from the wind and the rated power of the turbine:

$$P_{av_i} = \min(\frac{1}{2}\rho A v_i^3 C_{pmax}, P_{rated}) \tag{3.3}$$

The $C_{p,max}$ of a turbine depend on the aerodynamic efficiency of the turbine model and it is inferior to the $C_{p,Betz}$, presented in (2.2), which is a theoretical limit.

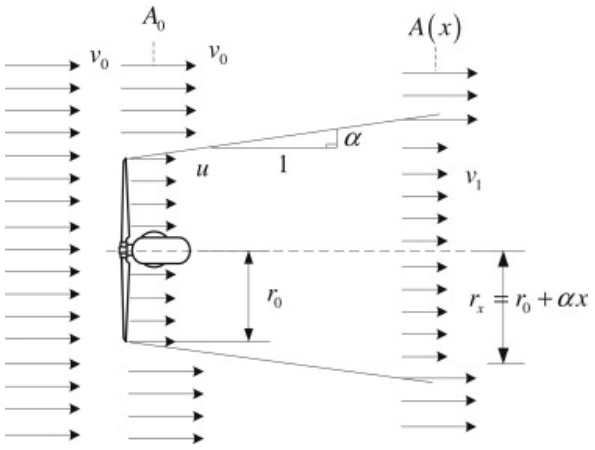

Figure 3.1: Jensen wake model [29]

It can be seen that the available power depend on the wind speed that the turbine faces, which in a wind farm also depend on the wake effect produced by the other turbines. The wind deficit produced by the wake can be calculated with different approaches (Section 2.2.1).

3.1.1 Wake model

To consider the interaction between the turbines within a wind farm, the disturbance on the wind speed that reaches the downstream turbines, known as wake effect, this work will refer to a relatively simple model based on estimations, known as the Jensen's model [15]. This model is based on the assumption of a linear expansion of the wake. If the near field behind the rotor is neglected, the wake can be treated as a turbulent wake. This feature comports that the radius r is proportional to downwind distance x. A balance of momentum gives (see Figure 3.1):

$$\pi r_0^2 u + \pi(r^2 - r_0^2)v_0 = \pi r^2 v_1 \tag{3.4}$$

Where u is the velocity behind the rotor, v_0 the free stream wind speed and v_1 the velocity in the wake at distance x. As a linear expansion is assumed, the wake can be represented as a cone which radius can be calculated as:

$$r_x = r_0 + \alpha x \tag{3.5}$$

where α is the entrainment coefficient and it is approximately 0.1 [15]. Solving (3.4) in terms of v_1 it can be obtained:

$$v_1 = v_0(1 - 2a\left(\frac{r_0}{r_x}\right)^2) \tag{3.6}$$

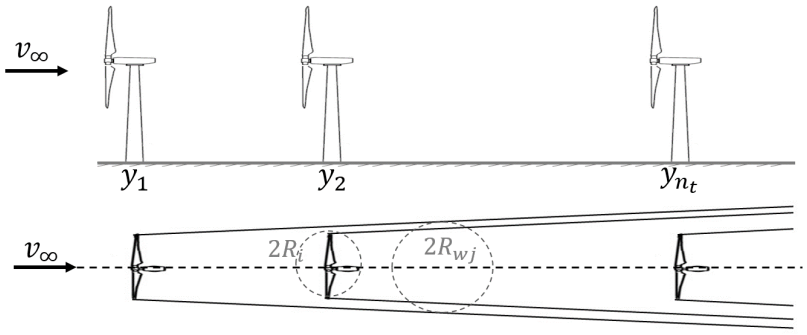

Figure 3.2: Wake effect for a row of wind turbines [28]

Where a is the induction factor and can be written as:

$$a = \frac{1 - \sqrt{1 - C_T}}{2} \tag{3.7}$$

with C_T the thrust coefficient of the turbine. As in a wind farm the downstream wind turbines experience multiple wake effects, as illustrated in Figure 3.2, the equation of the wind velocity in the wake for a downstream i wind turbine becomes:

$$v_i = v_\infty \left(1 - 2 \sum_{j \in \mathcal{N}: x_j < x_i} ((1 - \sqrt{1 - C_{T,j}}) k_{j,i}) \right) \tag{3.8}$$

where $\mathcal{N} = \{1, ..., n_t\}$ and $k_{ji} = (2R/(2R + 2\alpha(y_i - y_j)))^2$ with y_i and y_j are the position of the upstream and downstream turbine respectively.

3.2 Motivation of MPC

The wind farm controller, employed in the optimization problem that this work aims to solve, is based on a MPC strategy.

MPC is an optimization-based technique that computes an optimal control sequence aiming to minimize a cost function limited by physical and/or operational constraints. The advantages of this control strategy and the reasons why MPC is widely used in industrial application are the capacity of handling multivariable control problems, the possibility to take account of a set of constraints and to allow operation closer to them (compared with conventional controllers), and the low control update rates [30]. Especially, the possibility to consider constraints into the control strategy is important in the process industry for the profitability of the operations. These constraints are often associated with direct costs, i.e.

the heat required for manufacturing a product, and running a process at one ore more constraints is generally more profitable. At the same time constraints on the control signals can also be present. Usually this type of constraint is in form of saturation, i.e. maximum flow rate due to pipe diameters, or in form of rate constraints, i.e. limited slew rates of valves and other actuators [30].

3.3 MPC strategy description

The formulation of the controllers is usually designed by using a state-space model of the system in discrete time [30], [31]. For instance, the formulation of a discrete-time model of a general system can be given by:

$$\dot{\mathbf{x}}(k+1) = \mathbf{A}\mathbf{x}(k) + \mathbf{B}\mathbf{u}(k) \tag{3.9}$$

where $k \in \mathbb{Z}_{\geq 0}$ denotes the discrete time. The vectors $x \in \mathcal{X} \subseteq \mathbb{R}^{n_x}$ and $u \in \mathcal{U} \subseteq \mathbb{R}^{n_u}$ represent, respectively, the system states and the control inputs, both subject to the physical and/or operational set of constraints $\mathcal{X}$ and $\mathcal{U}$. Let

$$\hat{\mathbf{u}}(k) \triangleq \big(\mathbf{u}(k|k), \mathbf{u}(k+1|k), ..., \mathbf{u}(k+H_p-1|k)\big) \tag{3.10}$$

be a feasible control input sequence over a fixed-time prediction horizon $H_p \in \mathbb{Z}_{>0}$. Also, let

$$\hat{\mathbf{x}}(k) \triangleq \big(\mathbf{x}(k+1|k), \mathbf{x}(k+2|k), ..., \mathbf{x}(k+H_p|k)\big) \tag{3.11}$$

be the system state sequence that is generated by applying the control input sequence $\hat{\mathbf{u}}(k)$ to the system. Finally, the strategy aims to solve an open-loop finite-horizon multi-objective optimization problem in the general form of:

$$\underset{\hat{\mathbf{u}}(k)}{\text{minimize}} \quad J(\mathbf{x}_k, \mathbf{u}_k) = \sum_{m=1}^{n} \sum_{j=0}^{H_p-1} \gamma_m J_m \left(\mathbf{x}_{k+j|k}, \mathbf{u}_{k+j|k}\right) \tag{3.12a}$$

subject to (3.12b)

$$\mathbf{x}_{(k+j+1|k)} = \mathbf{A}\mathbf{x}_{(k+j|k)} + \mathbf{B}\mathbf{u}_{(k+j|k)} \qquad j \in [0, H_p] \cap \mathbb{Z}_{\geq 0} \tag{3.12c}$$

$$\mathbf{x}_{(k+j|k)} \in \mathcal{X} \qquad j \in [0, H_p] \cap \mathbb{Z}_{\geq 0} \tag{3.12d}$$

$$\mathbf{u}_{(k+j|k)} \in \mathcal{U} \qquad j \in [0, H_p - 1] \cap \mathbb{Z}_{\geq 0} \tag{3.12e}$$

where J determines the cost function through the prediction horizon H_p and being J a multi-objective function, it is defined as the sum of the individual n cost functions J_m. Additionally, the parameter $\gamma_m \in \mathbb{R}_{\geq 0}$, is a weight that allows the prioritization of the objectives.

Assuming that the optimization problem is feasible, there is an optimal control input sequence given by:

$$\hat{\mathbf{u}}_k^* \triangleq \left(\mathbf{u}_{k|k}^*, \mathbf{u}_{k+1|k}^*, ..., \mathbf{u}_{k+H_p-1|k}^*\right) \tag{3.13}$$

As the receding horizon philosophy only allows to apply to the system the first control input from the optimal sequence [30], the final control input is $\mathbf{u}^*(k|k)$. The new state of the system is then calculated, and the iterative procedure repeated for the next discrete time step, where a new final control input is computed and so on.

3.4 Problem formulation

The principal objective of the central controller of a wind farm is to meet the power demand required by the TSO at any moment. Once ensured the tracking of the power demand, an additional degree of freedom is left, which is the individual power contribution of each turbine, and can be used to satisfy other requirements. For the purpose of this work, in the context of grid frequency support, different WTs active power contributions have been tested in order to find the most suitable one for the maximization of the wind farm power reserve.

For these reasons, the control objectives considered in the formulation of the MPC are:

1. Tracking of the power demand profile P_{dem} set by the TSO, formulated as the minimization of the cost function:

$$J_1 = \|P_{dem} - \sum_{i=1}^{n} P_{g,i}\|_2 \tag{3.14}$$

   where P_{dem} is an external input and $P_{g,i}$ the power generated by each turbine.

2. Distribution of the active power set points within the wind farm, with the minimization of the cost function:

$$J_2 = \|W\ P_r\|_2 \tag{3.15}$$

   with W the weighing matrix, corresponding to the degree of freedom, different for each of the control strategies. The selection of the weights will be explained in Section 3.5.

3. Minimization of the variation of the control action aiming to avoid undesired peaks in the output power signal:

$$J_3 = \|\Delta P_r\|_2 \tag{3.16}$$

The final objective function can be seen as the sum of these three cost functions multiplied for a coefficient (3.17). These coefficients are used to prioritize the objectives within the cost function as the different objectives are not equally important. In this case the priority is set on the tracking of the power demand (Objective 1) and therefore the coefficient α will be higher than the others. In order to have the MPC meeting all the requirements, and with the priority desired, a tuning of the coefficients' values need to be performed.

$$J = \alpha J_1 + \beta J_2 + \gamma J_3 \tag{3.17}$$

In order to formulate the state the multi-objective problem using the MPC technique, it is assumed that the power response of a wind turbine can be modelled as a first order system [28], defined as:

$$\dot{P}_g = \frac{P_r - P_g}{\tau} \tag{3.18}$$

where P_r is the power set-point sent by the wind farm controller, P_g the generated power and τ the time constant of the first order system. Therefore, the state space model of the system, needed for the MPC formulation (Section 3.3), can be defined as:

$$\dot{\mathbf{x}}(t) = \mathbf{A}\mathbf{x}(t) + \mathbf{B}\mathbf{P}_r(t) \tag{3.19}$$

where $\mathbf{x} = [P_{g,1}, P_{g,2}, ...P_{g,n_t}]^T$ is the state vector of generated power, $\mathbf{P}_r = [P_{r,1}, P_{r,2}, ..., P_{r,n_t}]$ is the vector of the control actions with the values of power reference, $\mathbf{A} = [-\frac{1}{\tau}\mathbf{I}_{n_t}]$ and $\mathbf{B} = [\frac{1}{\tau}\mathbf{I}_{n_t}]$ the diagonal matrices being $\mathbf{I}$ the identity matrix and n_t the number of wind turbines.

As the MPC works with discrete variables the state space model needs to be discretized for a sampling time T_s, resulting in:

$$\dot{\mathbf{x}}(k+1) = \mathbf{A}_d\mathbf{x}(k) + \mathbf{B}_d\mathbf{P}_r(k) \tag{3.20}$$

with $k \in \mathcal{N}$ the discrete time constant and $\mathbf{A}_d,\ \mathbf{B}_d$ the discrete versions of matrices $\mathbf{A}$ and $\mathbf{B}$. It has been seen that in MPC formulation control actions and system state can be controlled to respect physical and desired operational limits. In this problem formulation the set of

constraints is applied only on the control inputs and is defined as:

$$\mathcal{U} = \left\{ \mathbf{P}_r \in \mathcal{R}^{n_t} | \mathbf{P}_r(k) \in [\mathbf{P}_{min}, \mathbf{P}_{max}], \forall k \right\} \tag{3.21}$$

where the minimum value of power reference is set for all the turbines to 1 MW, to not occur in a shutdown of the wind turbines, while $\mathbf{P}_{max} = [P_{av,1}, ..P_{av,n_t}]$ is the vector of the available power at each wind turbine.

According with the control strategy presented in Section 3.3, let the sequence of feasible control inputs $\hat{\mathbf{u}}(k)$ and the sequence of feasible states $\hat{\mathbf{x}}(k)$ within the prediction horizon $H_p \in \mathcal{N}_{>0}$ be

$$\hat{\mathbf{u}}(k) = \left\{ \mathbf{P}_r(k|k), ..., \mathbf{P}_r(k + H_p - 1|k) \right\} \tag{3.22a}$$

$$\hat{\mathbf{x}}(k) = \left\{ \mathbf{x}(k+1|k), ..., \mathbf{x}(k + H_p|k) \right\} \tag{3.22b}$$

Hence, the formulation of the multi-objective optimization problem that the MPC has to solve is:

$$\underset{\hat{\mathbf{u}}(k)}{\text{minimize}} \quad J(k) = \sum_{i=0}^{H_p - 1} J(k+i) \tag{3.23a}$$

subject to (3.23b)

$$\mathbf{x}(k+j+1|k) = \mathbf{A_d}\mathbf{x}(k+j|k) + \mathbf{B_d}\mathbf{u}(k+j|k) \qquad j \in [0, H_p] \cap \mathbb{N} \tag{3.23c}$$

$$\mathbf{u}(k+j|k) \in \mathcal{U} \qquad j \in [0, H_p - 1] \cap \mathbb{N} \tag{3.23d}$$

If the problem is feasible , the MPC output is the optimal sequence:

$$\hat{\mathbf{u}}_{opt}(k) = \left\{ \mathbf{P}_{r,opt}(k|k), ..., \mathbf{P}_{r,opt}(k + H_p - 1|k) \right\}. \tag{3.24}$$

For the receding horizon philosophy the input applied to the system is the first element of optimal sequence, which correspond to $\mathbf{P}_{r,opt}(k|k)$. and perform a new measurement of the state vector. At this point the optimization problem is repeated and solved for the next discrete time step k till the end of the simulation time.

3.5 Weighing matrix

To analyse the effect of the power contribution of each WT within a wind farm on the total primary reserve, different formulation of the cost function presented in (3.16) were tested.

To build the weighing matrix W, three distribution were taken into consideration in order to find the most suitable for the maximization of the power reserve. The three distribution are the following:

- **Proportional distribution** - The power set point of each WT is proportional to the available power calculated at the rotor height (3.25). This approach is used by the authors of [25] and [32].

$$P_{ref_i} = \frac{P_{av_i}}{P_{av_{tot}}} * P_{dem} \tag{3.25}$$

  Where $P_{av_{tot}}$ is the sum of the individual available power of the turbines within the wind farm and P_{av_i} is calculated as in (3.3).

- **Equal distribution** - The power requirement of the wind farm is equally distributed among the n WTs, respecting the limits of available power of each one.

$$P_{ref_i} = \frac{P_{dem}}{n} \tag{3.26}$$

- **Backward distribution** - This approach aims to maximize the power produced by the downstream wind turbines and to reduce the contribution of the upstream ones, in order to mitigate the wake effect and increase the power reserve.
  For example, considering the wind turbine row shown in Figure 3.2, with v_∞ the wind free stream velocity and direction, the desired distribution of the power contribution would be described as:

$$P_{ref,y_{nt}} > ... > P_{ref,y_2} > P_{ref,y_1} \tag{3.27}$$

Chapter 4

Simulations and Results

4.1 Simulation set-up

To evaluate the effects of the different control strategies a wind farm was created with SimWindFarm toolbox [32], which uses the dynamic wake meandering model to estimate the wake effects according with the wind turbine layout and the ambient turbulence. All the simulations have been run on Simulink and Matlab 2018b.
The layout of the wind farm, presented in Figure 4.2, is composed by three row of five turbines NREL 5MW, which have a rotor diameter of 126 meters and are spaced evenly 630 meters ($5D$). The wind field size was 5000 x 3500 m^2 and the grid spaced 15 m. Simulation were performed in laminar flow conditions, with turbulence intensity set equal to 0.
For the formulation of the MPC the Matlab tool YALMIP [33] with the optimization solver Gurobi 8.1.1 were used.
Several simulations were performed for each of the control formulations, considering different power demands in de-loading operation, at a constant wind speed but with different directions. To simulate the different wind direction the layout of the wind farm was rotated.

The cases presented in Table 4.1 were assumed.

Since the turbines are required to regulate power on a millisecond scale, the sample time T_s and the prediction horizon H_p have been set to a relatively small value.

Furthermore, the coefficients α, β, γ of the cost function (3.17), have been found through an iterative tuning, performed manually.

Wind speed	11 m/s
P_{dem}	From 55% to 95% of P_{max} in steady state conditions (with 5% steps)
Wind speed direction	0°, 30°, 45°, 60°, 90°
Simulation time	700 seconds
Sample time T_s	0.08 seconds
Prediction horizon H_p	3
Time constant τ	0.1
α	5
β	1
γ	0.001

Table 4.1: Setting of the simulation parameters

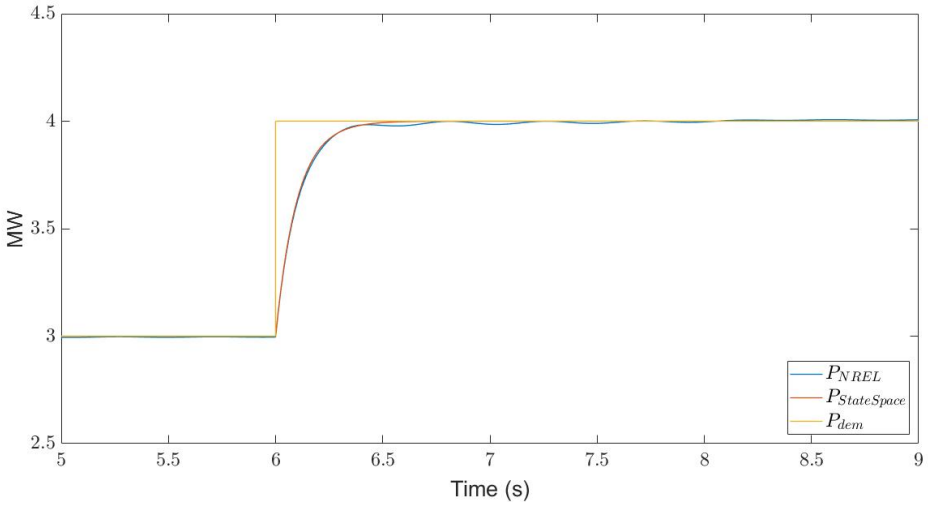

Figure 4.1: Response of the NREL 5 MW wind turbine and the state space model with $\tau = 0.1$

Finally the time constant τ was calculated applying a step from 3 MW to 4 MW in power demand to the simplified model of wind turbine NREL 5 MW and comparing the response with the one of the state space model described in (3.19) for a single wind turbine. The time constant which best approximated the behaviour of the NREL 5 MW was $\tau = 0.1$ s. The response of the system is shown in Figure 4.1.

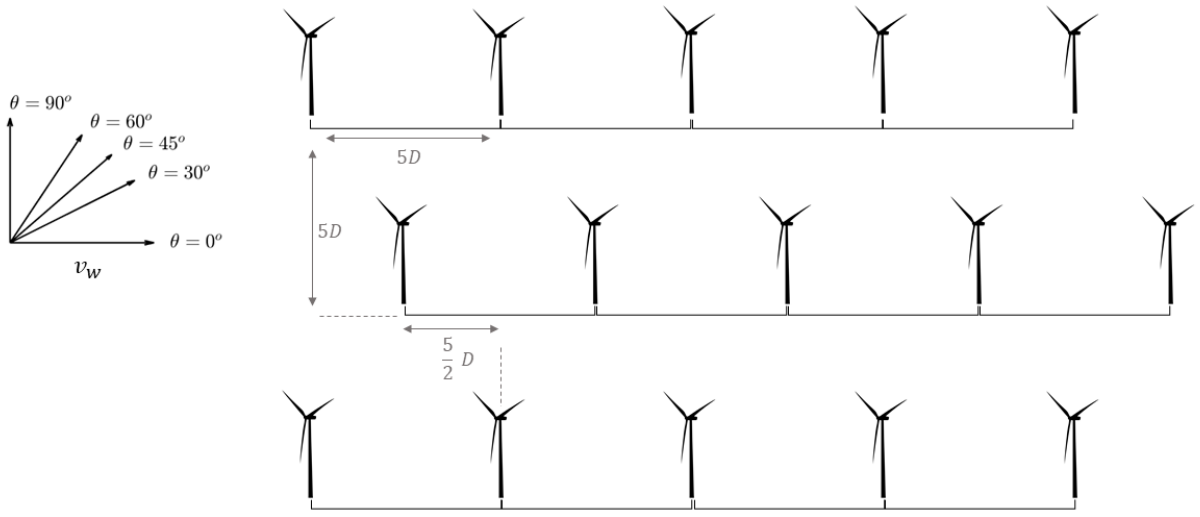

Figure 4.2: Layout of the wind farm and wind directions

4.2 Case study

The case of a wind direction of 60° and step in power demand from 55% to 60% of the available power in steady state conditions P_{av}^{ss}, will be taken as an example to present the results of the simulations. The value P_{av}^{ss} correspond to the maximum power that can be generated from the wind farm under certain wind speed and direction at steady state condition, that means after the time needed by the wake to expand and reach the other turbines. In this case $P_{av}^{ss} = 56$ MW.

As the wind direction can not be modified in SimWindFarm, the layout of the wind farm is rotated of 60°. The wake produced by the wind turbines can be seen in Figure 4.3. At $t_1 = 300$ s the overall power demand P_{dem} raise from 30.8 MW to 33.6 MW meeting the 60% of the maximum power production of the wind farm under these wind conditions. For the all the control strategies the first objective, the tracking of the power demand, is met as shown in Figure 4.4.

4.2.1 Proportional distribution

In the control strategy based on the proportional distribution the weights have been set, as shown in Figure 4.5, to prioritize the power contribution of the upstream WTs, which have the highest available power. WT_{11}, WT_{12}, WT_{13}, WT_{14}, WT_{15} and WT_1, which face the

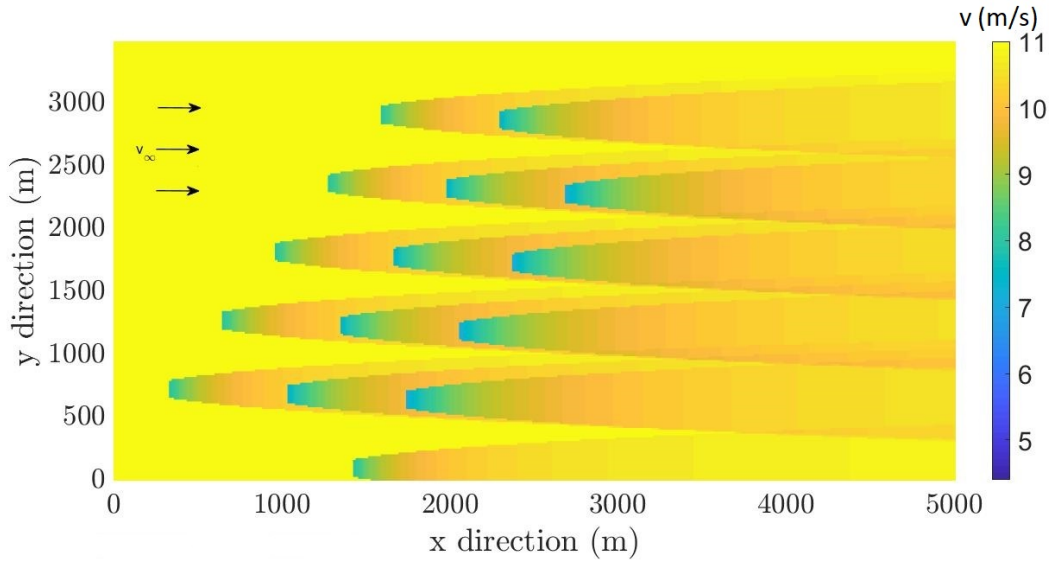

Figure 4.3: Wind field simulated with SWF for a direction of $\theta = 60^o$ and $v_\infty = 11$ m/s

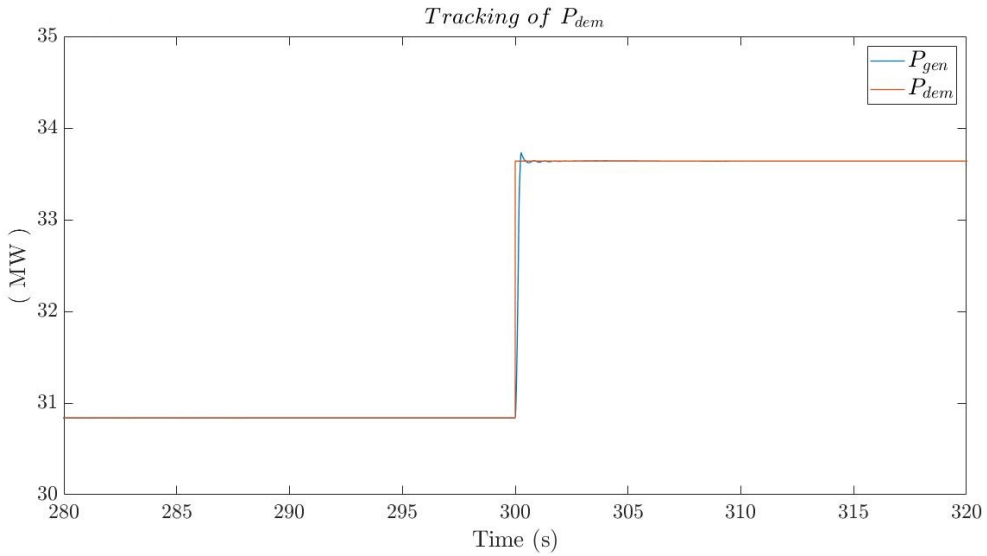

Figure 4.4: Tracking of the step in power demand

free stream wind speed, will have the highest power setpoint, while the downstream WTs (WT_2, WT_3, WT_4, and WT_5), which experience the wake of the other turbines and therefore a significant wind speed deficit, will have the lowest power setpoint. The response of the wind farm under the MPC strategy is shown in Figure 4.6 and follows the individual power distribution set by the weighing matrix.

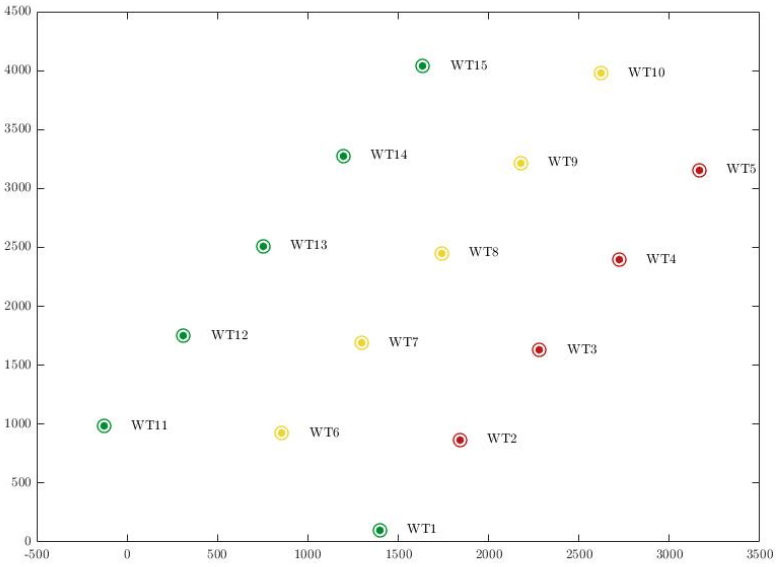

Figure 4.5: Proportional weights distribution within the wind farm.

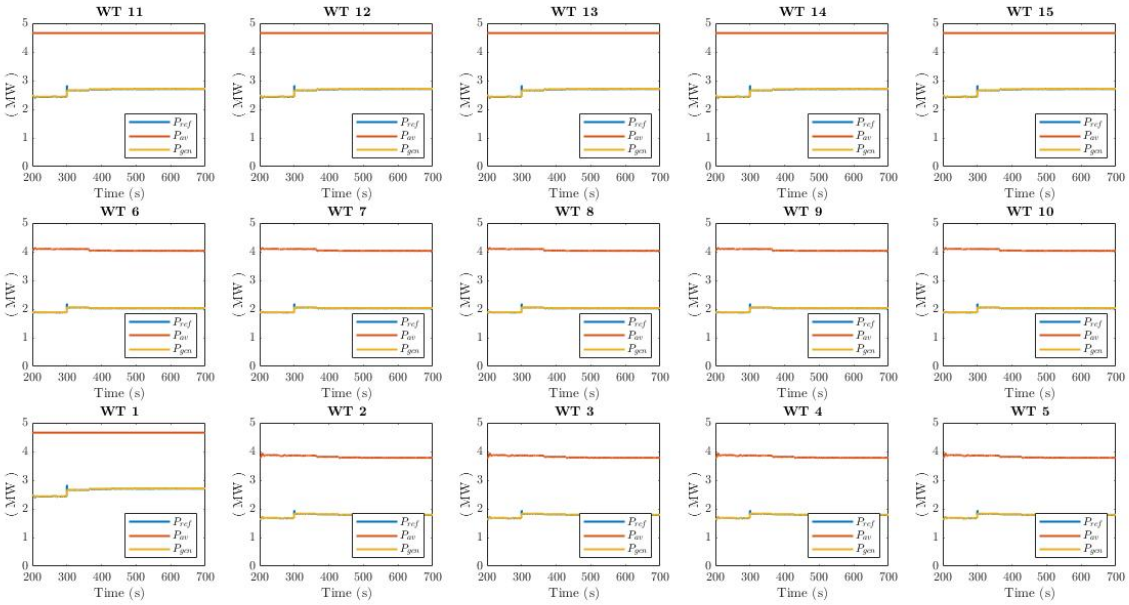

Figure 4.6: Available and generated power of each turbine of the wind farm under the proportional distribution

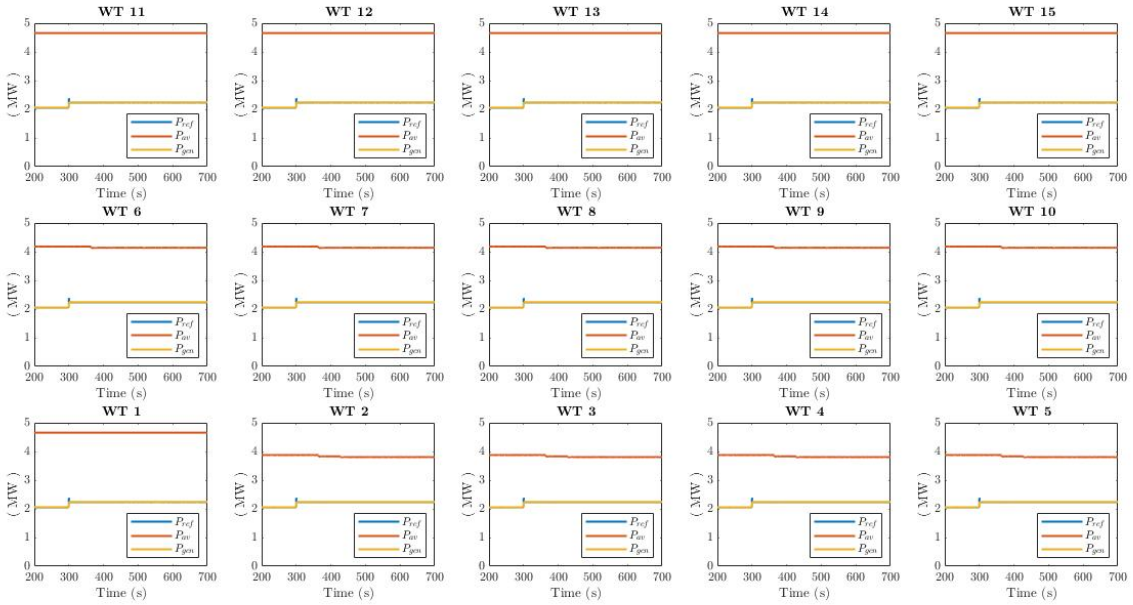

Figure 4.7: Available and generated power of each turbine of the wind farm under the equal distribution

4.2.2 Equal distribution

In this control approach the wake effect is not considered in the formulation of the MPC and the power demand is equally distributed among all the turbines. As there are not limits in power available for the downstream wind turbines the power set point is the same for all the wind turbines, Figure 4.7.

4.2.3 Backward distribution

The objective of this approach is to prioritize the contribution of the most downstream WTs and keep at the minimum operation the upstream ones in order to reduce their wake. For this purpose WT_1, WT_2, WT_3, WT_4, WT_5 and WT_{10}, which wake doesn't affect any other turbine, will have the highest power contribution (Figure 4.8). On the other hand WT_{11}, WT_{12}, WT_{13} and WT_{14}, which wake affects the downstream turbines, are kept at their minimum operating value of 1 MW, value that has been set to avoid the shutdown of the turbines. The response of the wind farm and the individual power contributions can be seen in Figure 4.9.

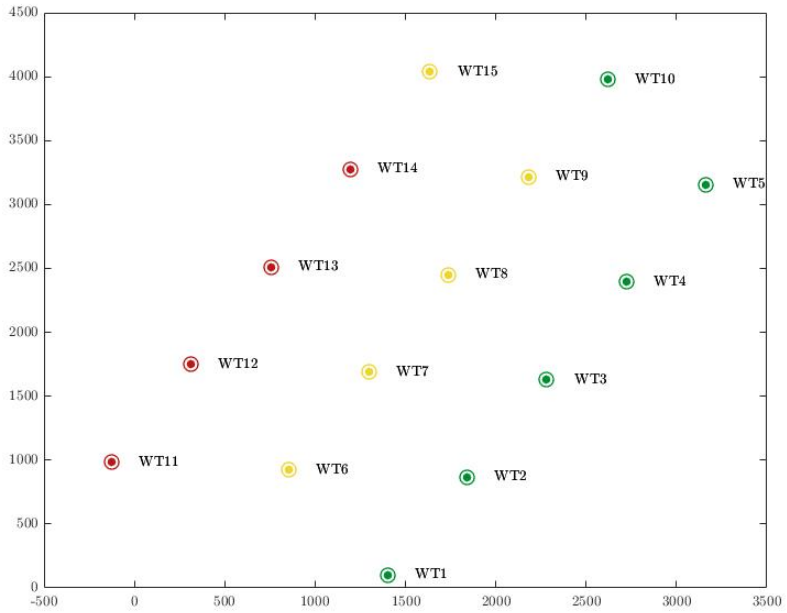

Figure 4.8: Backward weights distribution within the wind farm.

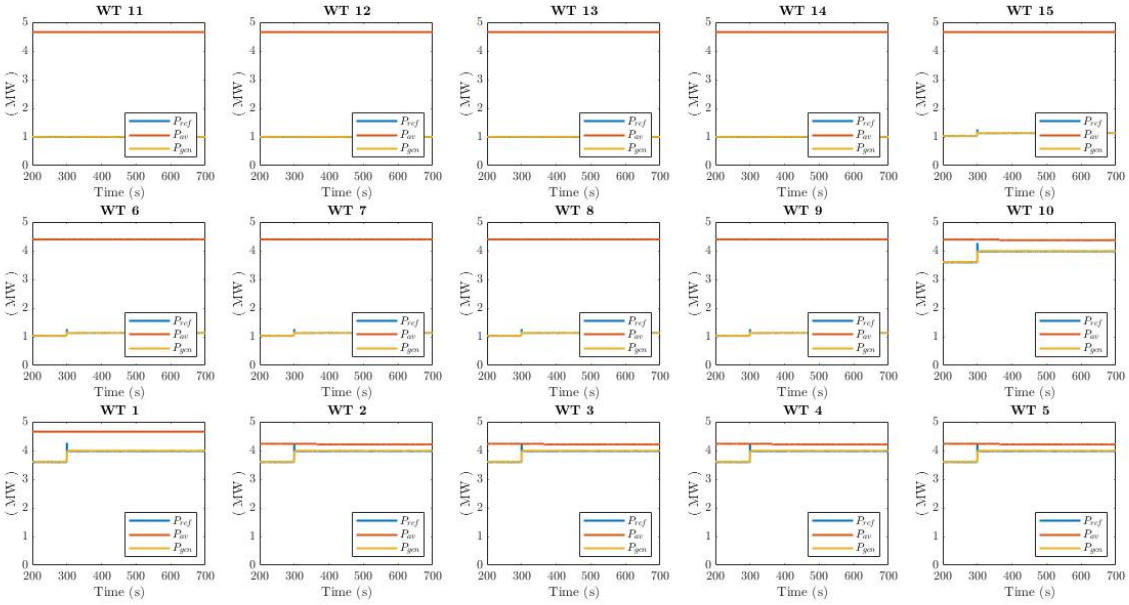

Figure 4.9: Available and generated power of each turbine of the wind farm under the backward distribution

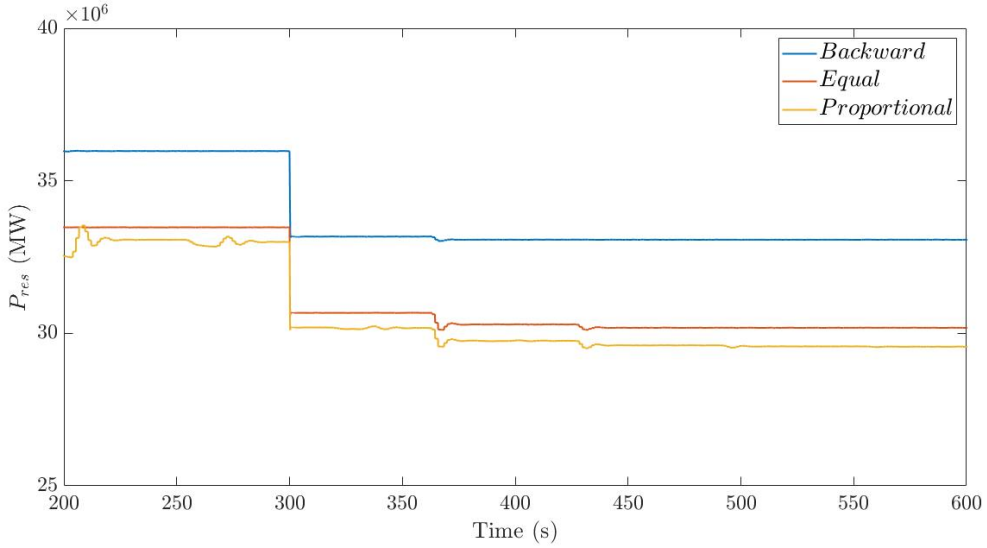

Figure 4.10: Power reserve under the three control strategies.

4.2.4 Comparison

It has been seen in Figure 4.4 that the power demand required by the TSOs is met in all the control strategies. Focusing on the power reserve, which depends on the second objective of the optimization, and therefore on the individual power contribution of the WTs, it can clearly be seen, Figure 4.10, that for the case analysed the backward distribution has a significantly higher value of power reserve.

4.3 Results

The same simulation has been run for all the cases mentioned previously, changing the power demand set point and the wind direction. The value of power reserve obtained are illustrated in Figure 4.11.

The major improvements in power reserve with the use of the backward distribution compared to the other strategies happen when the wake effect is strong, due to the proximity of the turbines in the wake. In Figure 4.12 the different wake expansions, based on the wind direction, are compared. It can be seen that for the case of $\theta = 0^o$ and $\theta = 60^o$ the second wind turbine is located, according with the wake direction, close to the first one and therefore it experiences a significant wind speed deficit. For those cases, the decrease in power generation of the first turbine, produce a considerable decrease of the wake effect and an

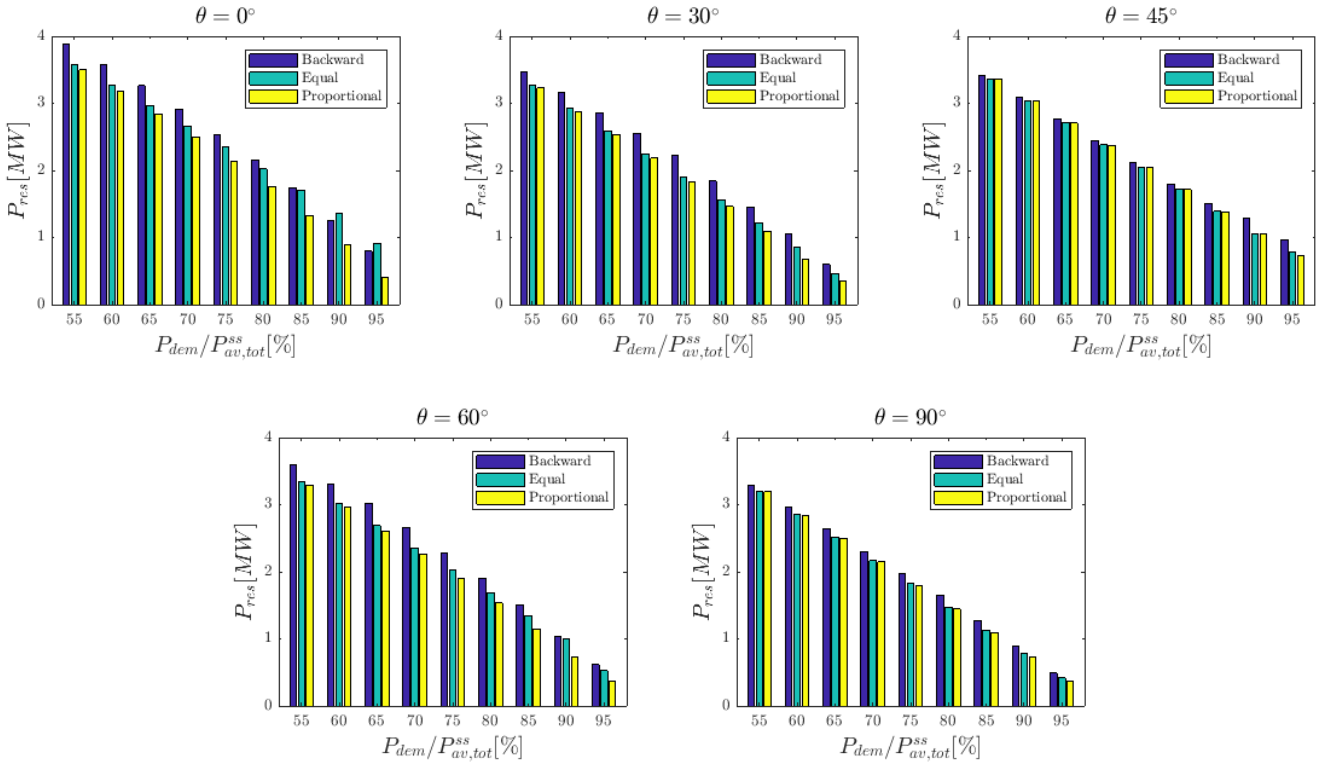

Figure 4.11: Comparison of the three control strategies under several operation set points and wind directions.

increase in power reserve. At the same time for power demands close to the available power in steady state conditions, for the case of $\theta = 0^o$ it can be noticed that the best configuration becomes the equal distribution. To understand this results the power contribution of a row of the wind farm is presented in Figure 4.13 for both the backward and equal distribution. For power demands close to the $P^{ss}_{av,tot}$ the deloading of the first turbine produce a big wake reduction on the second turbine but also involves a greater power generated by the second and third turbine which implies an augmentation of their wake. This results in an higher wind speed deficit for the other downstream turbines. On the other hand, if the deloading is equally split among the first, second and third turbine the wind deficit experienced by the other turbines is less significant and therefore the power reserve is higher. This happens only for the case of $\theta = 0^o$ because the turbines in the wake direction are the closest to each others. For the other cases, especially $\theta = 45$ and $\theta = 90^o$, as the turbine in the wake is placed very far from the upstream one, the wind speed deficit is not significant due to the wake recovery and there is no main difference among the three control strategies proposed. Still it can be seen that the backward distribution is slightly better.

Furthermore the numeric value of the power reserve is higher for the cases of stronger wakes ($\theta = 0$ and $\theta = 60^o$). However this is due to the fact that the values of $P^{ss}_{av,tot}$ are different

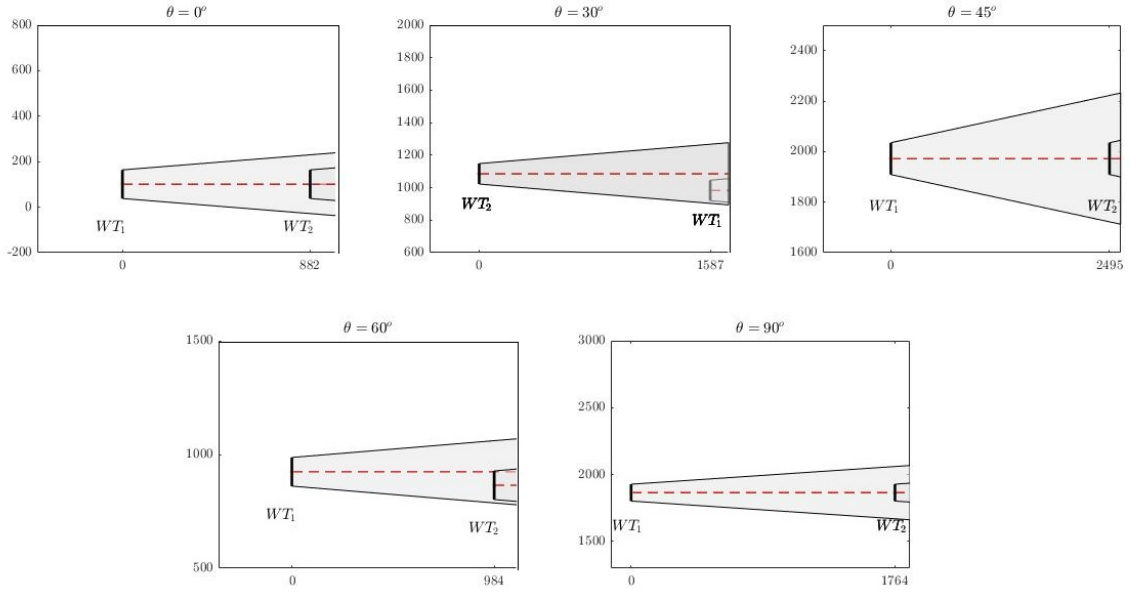

Figure 4.12: Wake effect between two turbines depending on the wind direction.

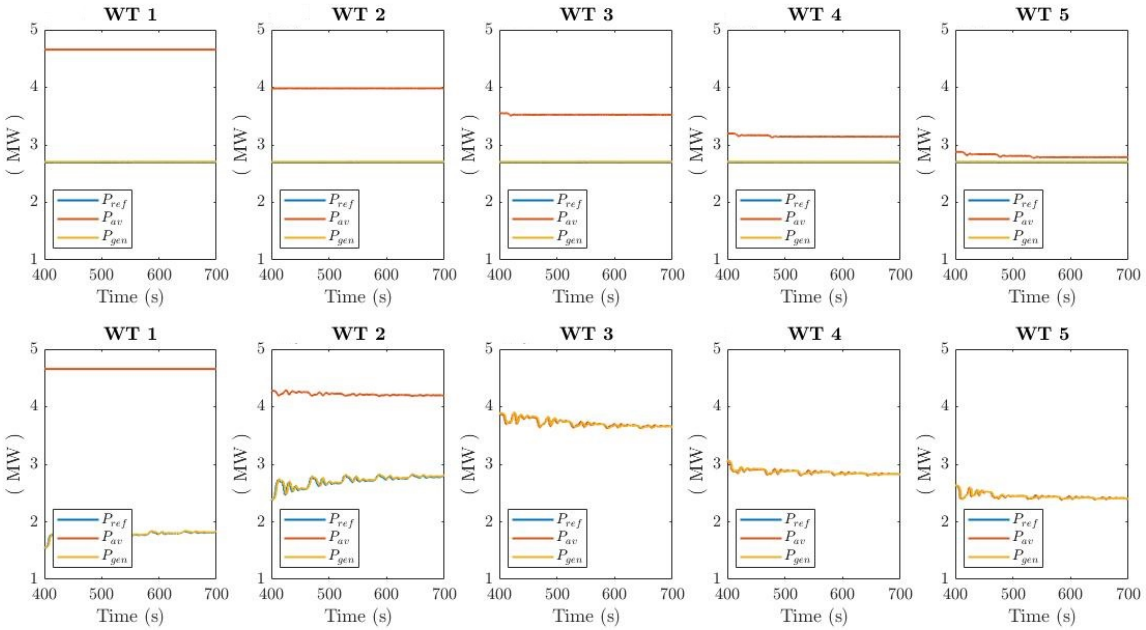

Figure 4.13: On top: Distribution of the generated power among a row of wind turbines under the equal distribution strategy. At the bottom: Distribution of the generated power under the backward distribution strategy.

for the different wind directions and, as the power setpoint is a percentage of it, it is not significant to compare the values of power reserve among the different wind direction case studies as they refer to different values of power demands.

Chapter 5

Reactive power control

5.1 MPC for Reactive Power Control

In the context of ancillary services, wind farm are also required, a part from providing frequency support, to follow technical requirements of voltage support set by the TSOs. Generally the grid codes requires the reactive power capability of the wind farm and to maintain the voltage within the operating range at the PCC [34]. The voltage regulation in wind farm is related to the reactive power control.

Despite different control modes typically used for the purpose of providing reactive power control, such as reactive power set-points or power factor regulations, the voltage control mode shows better performance for transmission systems [35].

Several control modes used in literature are presented in [34]. Among them, MPC has been used in several studies for voltage control [34] [35], [36], as it brings some advantages compared to the classical control strategies. The advantages of using MPC are:

- A combined active and reactive power control in case of voltage deviations. As the Var capacity of a wind turbine converter depends on the active power generated, it is useful to be able to control active power set points of the wind turbines in order to increase the voltage support capability of the wind farm. However, in the conventional wind farm control, active and reactive power are controlled separately [36].

- The possibility of controlling active and reactive power with different time constants [36]. While the active power time constant is around 0.1 seconds, generally the reactive

power response time of wind turbines is in the range of 1 ~10 s [34].

5.2 Problem formulation

Considering the requirement of voltage support, a new objective need to be added to the controller structure presented in section 3.4. Hence, a part from ensuring the tracking of the power demand while maximizing the primary reserve, the wind power plant controller has to keep the voltage at the PCC within the operation range.

Therefore the new set of objectives considered in the MPC formulation is:

1. The minimization of the voltage deviations at the the PCC from the set point set by the TSO:

$$J_1 = \|\Delta V_{pcc}\|_2 = \|V_{pcc}^0 + \sum_{i=1}^{n} \frac{\partial V_{pcc}}{\partial P_{WT,i}} \Delta P_{WT,i} + \sum_{i=1}^{n} \frac{\partial V_{pcc}}{\partial Q_{WT,i}} \Delta Q_{WT,i} - V_{pcc}^{ref}\|_2 \quad (5.1)$$

   where $\partial V_{pcc}/\partial P_{WT,i}$ and $\partial V_{pcc}/\partial Q_{WT,i}$ are the voltage sensitivity coefficients, V_{pcc}^0 the measured voltage at the PCC and V_{pcc}^{ref} the reference voltage set by the TSOs.

2. The tracking of the power demand profile P_{dem} set by the TSO can be formulated as :

$$J_2 = \|P_{dem} - \sum_{i=1}^{n} \left(P_{g,i}^0 + \Delta P_{g,i}\right) \|_2 \quad (5.2)$$

   where $P_{g,i}^0$ is the measured power generated and ΔP_i the increase or decrease in power generation.

3. Distribution of the active power set points within the wind farm:

$$J_3 = \|W \left(P_{g,i}^0 + \Delta P_{r,i}\right) \|_2 \quad (5.3)$$

   Where $\Delta P_{r,i}$ the increase or decrease in power generation set point set by the controller. In this MPC formulation the backward distribution (3.27) for the construction of the weighing matrix W is adopted, as it was proved by the results (section 4.3) that in almost all the cases it is the best approach for the maximization of the power reserve.

4. Minimization of the variation of the control action aiming to avoid undesired peaks in the output power signal:

$$J_4 = \|\Delta P_r(k+1) - \Delta P_r(k)\|_2 \quad (5.4)$$

To conclude, the final multi-objective cost function is the sum of the four over-mentioned cost functions multiplied for a prioritization coefficient:

$$J = \alpha J_1 + \beta J_2 + \gamma J_3 + \delta J_4 \tag{5.5}$$

The system can be expressed with two different first order systems, one related to active power and one to reactive power, due to the different time constants:

$$\dot{\Delta P_g} = \frac{\Delta P_r - \Delta P_g}{\tau_p} \tag{5.6a}$$

$$\dot{\Delta Q_g} = \frac{\Delta Q_r - \Delta Q_g}{\tau_q} \tag{5.6b}$$

Where τ_p and τ_q are the time constants representing, respectively, the active and reactive power response of the system.

Hence, the state space model, already in discrete time, is:

$$\dot{\mathbf{x}}(k+1) = \mathbf{A}\mathbf{x}(k) + \mathbf{B}\mathbf{u}(k) \tag{5.7}$$

where $\mathbf{x} = [\Delta P_{g,1}, ...\Delta P_{g,n_t}, \Delta Q_{g,1}, ...\Delta Q_{g,n_t}]^T$ is the state vector of increment of active and reactive power, $\mathbf{u} = [\Delta P_{r,1}, ...\Delta P_{r,n_t}, \Delta Q_{r,1}, ...\Delta Q_{r,n_t}]^T$ is the vector of the control actions with the reference values of power increment, while

$$\mathbf{A} = \begin{bmatrix} -\frac{1}{\tau_p}\mathbf{I}_{n_t} & \mathbf{0} \\ \mathbf{0} & -\frac{1}{\tau_q}\mathbf{I}_{n_t} \end{bmatrix} \qquad \mathbf{B} = \begin{bmatrix} \frac{1}{\tau_p}\mathbf{I}_{n_t} & \mathbf{0} \\ \mathbf{0} & \frac{1}{\tau_q}\mathbf{I}_{n_t} \end{bmatrix}$$

the diagonal matrices with dimensions $2n_t \times 2n_t$. The system is subject to the following constraints:

$$\mathcal{U} = \left\{ \begin{array}{c} \Delta P_r \in \mathcal{R}^{n_t} | \mathbf{\Delta P}_r(k) \in [\mathbf{P}_{min} - \mathbf{P}_{gen}, \mathbf{P}_{max} - \mathbf{P}_{gen}], \forall k; \\ \mathbf{\Delta Q}_r \in \mathcal{R}^{n_t} | \mathbf{\Delta Q}_r(k) \in [\mathbf{Q}_{min} - \mathbf{Q}_{gen}, \mathbf{Q}_{max} - \mathbf{Q}_{gen}], \forall k \end{array} \right\}$$

where the minimum value of active power $\mathbf{P}_{min}$ is set to 1 MW, while $\mathbf{P}_{max}$ is the vector of the available powers. The constraints on the reactive power $\mathbf{Q}_{max}$ and $\mathbf{Q}_{min}$ are calculated looking at the PQ capacity curve of the converter, which depends on the terminal voltage and active power [36]. The optimization problem that the MPC has to solve is, considering the new state space model, cost functions and constraints, the one presented in 3.23a.

Section (mm^2)	R (Ω/km)	L (mH/km)	C (μF/km)	Ampacity (A)
095	0.2478	0.420	0.161	358
150	0.1597	0.387	0.188	452

Table 5.1: Electrical Characteristics of the AC Submarine 33-kV XLPE Three-Core Cables Database

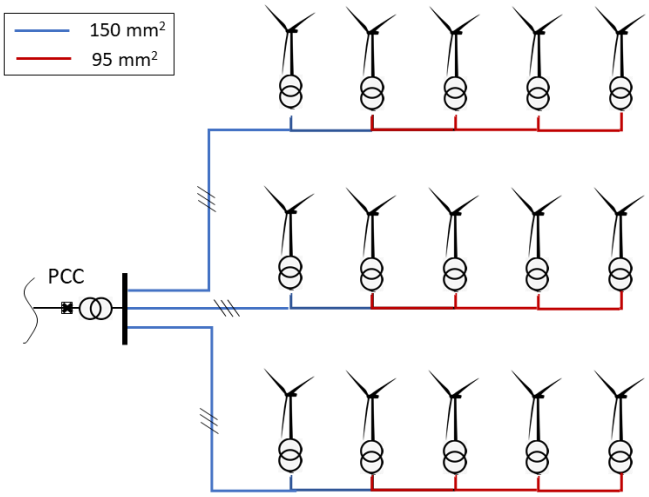

Figure 5.1: Wind farm layout

5.3 Simulation and results

5.3.1 Wind farm model

As the benchmark NREL 5 MW wind turbine model used in SimWindFarm [32], does not include a converter and the reactive power generation, for the purpose of this part of the study, a full-scale converter and its control block, inspired to the GE 3.6 MW [37], was added to the simplified model of NREL 5 MW.

The wind farm is composed by three row of five wind turbines, operating at 590 V. Each of the WTs row is connected to the PCC by a collector bus operating at 33 kV. Then, the collector buses are connected to the off-shore grid through a 33-120 kV transformer. The turbines are spaced 882 m, corresponding to 7 times the rotor diameter. The layout of the wind farm is presented in Figure 5.1. The selection of the cables was based on the AC submarine 33-kV XLPE three-core cables database [9]. The electrical characteristic can be seen in table 5.1.

Without the wind flow field estimated by SimWindFarm, the wind speed at each wind turbine, taking into account the wake effect, is dynamically calculated according to the (3.8), which is based on the Jensen's wake model. Through the wind speed, the power available at each wind turbine can be calculated as presented in (3.3).

5.3.2 Sensitivity coefficients

In order to be able to track the voltage required at the PCC, regulating active and reactive power, the cost function presented in (5.1) was defined referring to the sensitivity coefficient $\partial V_{pcc}/\partial P_{WT,i}$ and $\partial V_{pcc}/\partial Q_{WT,i}$. In literature, several examples of sensitivity analysis for power losses and voltage buses magnitude can be found, as the analysis is able to measure the impact of changing the system parameters on the system performances, and it is widely used for solving optimal power flows control problems [38]. Two main techniques are generally used in order to calculate the sensitivity coefficient: the Jacobian-based method, which uses an updated Jacobian matrix derived from the load flow problem, and the adjoint network method, based on the application of the Tellegen's theorem to the power network [39].

However, for the purpose of this study and the resources available, it was decided to calculate the coefficients in a experimental way, doing reasonable assumptions that would affect only marginally the performances of the controller. The idea behind the used approach is to change one parameter at the time, i.e. the active power of the WT 1, and look at the change in the voltage magnitude at the PCC in order to compute an analytical dependence between the quantities. The parameters that have been changed for the sensitivity analysis are the active and reactive power of each wind turbine.

Steps in active power of 0.1 p.u, from 0.2 to 1 p.u. were applied to the system, and, as an example of the behaviour of the system, the voltage response to changes in power generated by the WT1 can be seen in Figure 5.2.

Following the same method, for the reactive power dependence, the values of Q were changed from -1 p.u. to 1 p.u. with steps of 0.1 p.u, in Figure 5.3 the results of the analysis for changes in WT 1 reactive generation are presented.

As shown, the Q-V curve can be reasonably approximated with a linear function and therefore obtain a constant $\partial V_{pcc}/\partial Q_{WT,i}$ coefficient. For the case of the P-V curve, the dependence is not linear and should be modeled with a polynomial curve.

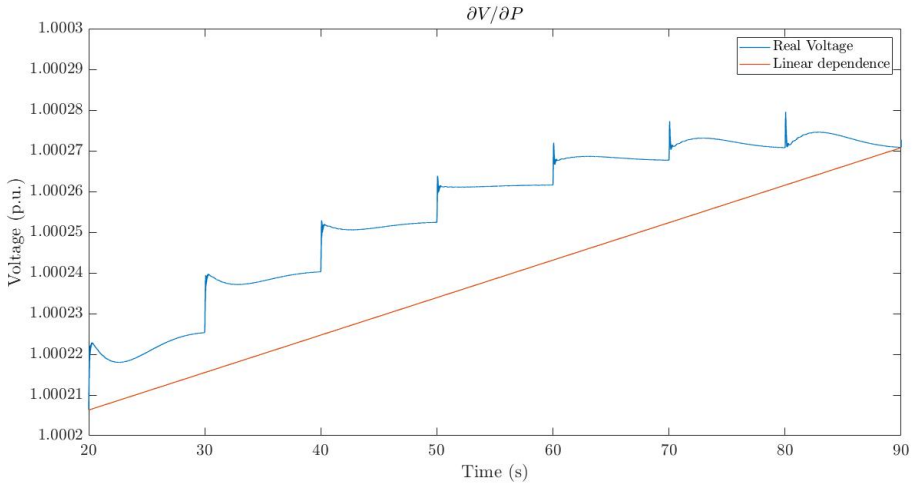

Figure 5.2: Sensitivity analysis of voltage magnitude with respect to active power of WT 1

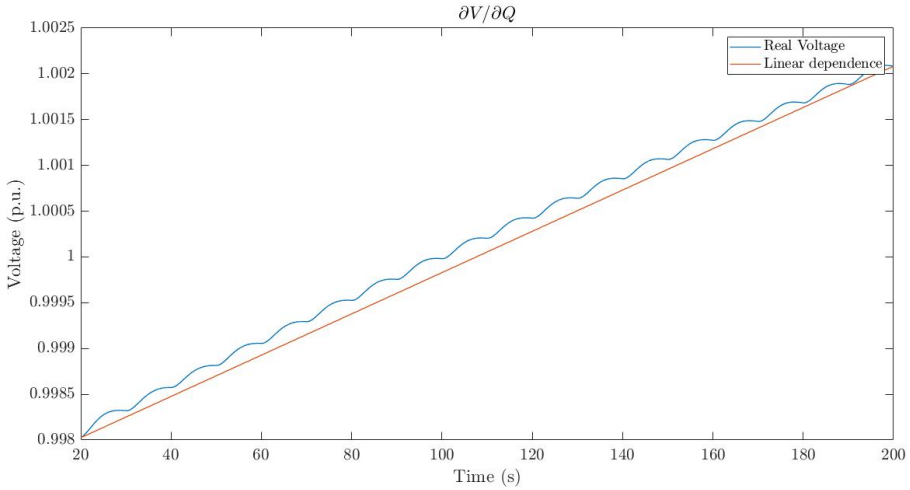

Figure 5.3: Sensitivity analysis of voltage magnitude with respect to reactive power of WT 1

However, as the voltage dependence on active power is considerably lower than the one on reactive power, it was considered acceptable to approximate the curve with a linear function, as the error introduced does not affect excessively the performances of the controller. Hence, $\partial V_{pcc}/\partial P_{WT,i}$ can also be considered constant.

The same procedure was applied to all the wind turbines of the wind farm.

5.3.3 Simulation set up

In order to validate the MPC formulation for the optimization problem presented in section 5.2, a simulation has been run in Simulink 2018b. To evaluate the voltage tracking performances of the controller, a three phase RLC load has been applied to the grid with

the objective of seeing the restoration of the voltage drop caused by the sudden increase of demand.

The simulation set-up is the following:

Wind speed	11 m/s
Wind direction	0^o
P_{dem}	Step from 30 MW to 40 MW at sec. 20
Load	P = 10 kW $Q_c = 10$ var $Q_L = 100$ var from 15 s to 25 s
α	10
β	5
γ	0.01
δ	1
τ_q	7 s
τ_p	0.1 s
Prediction Horizon H_p	3
Sample Time T_s	0.08
Simulation Time	35 s

Table 5.2: Simulation parameters set-up

Most of the parameters were kept equal to the ones used for the simulations of Section 4.1. The reactive time constant τ_q was arbitrarily chosen within the typical range used to model wind turbines response [34]. Furthermore, the delay in the wake expansion, which, for this kind of distance between the turbines, is usual around 60 s was set to 2 s in order to speed up the simulation. The coefficients $\alpha, \beta, \gamma, \delta$ were decided through a manual iterative tuning of the controller. To conclude, the active and reactive power of the load were chosen in order to have a voltage drop that the total reactive capacity of the wind farm would have been able to recover.

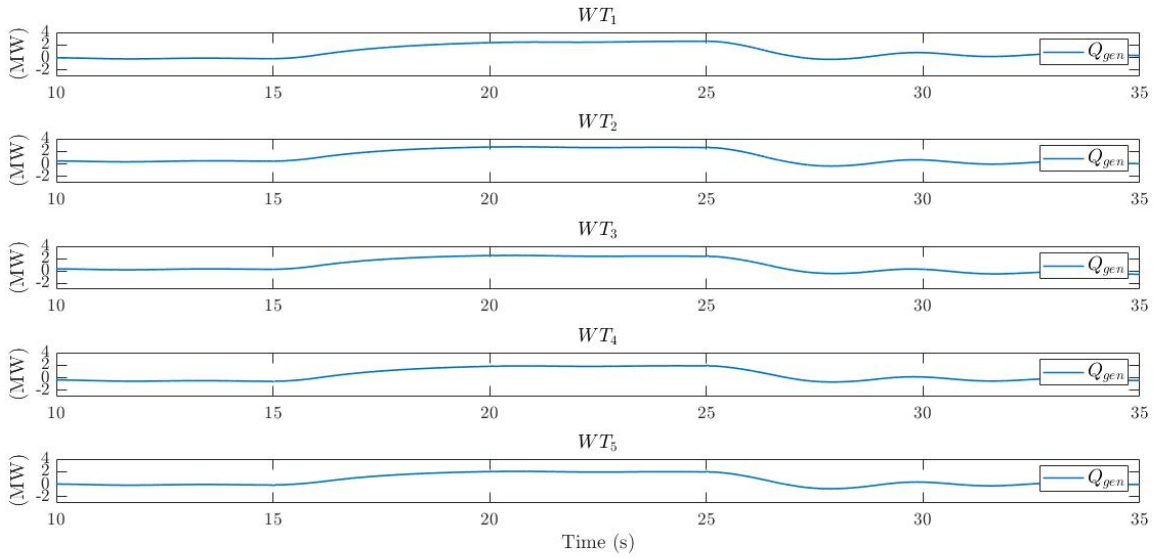

Figure 5.5: Reactive power contribution in a row of wind turbines

5.3.4 Results

The voltage set-point was set to 1 p.u., considering a base voltage equal to 120 kV. As it can be seen in Figure 5.4, once at 15 s the load is connected to the grid, the voltage drops to 0.98 p.u. and restored in 5 s by increasing the reactive power injection of the wind turbines, Figure 5.5. At 25 s, when the load is disconnected there is a sudden increase in the PCC voltage, that the controller manages to bring back to the reference value in a couple of seconds. However, in this case the output voltage presents an oscillating behaviour around the reference values.

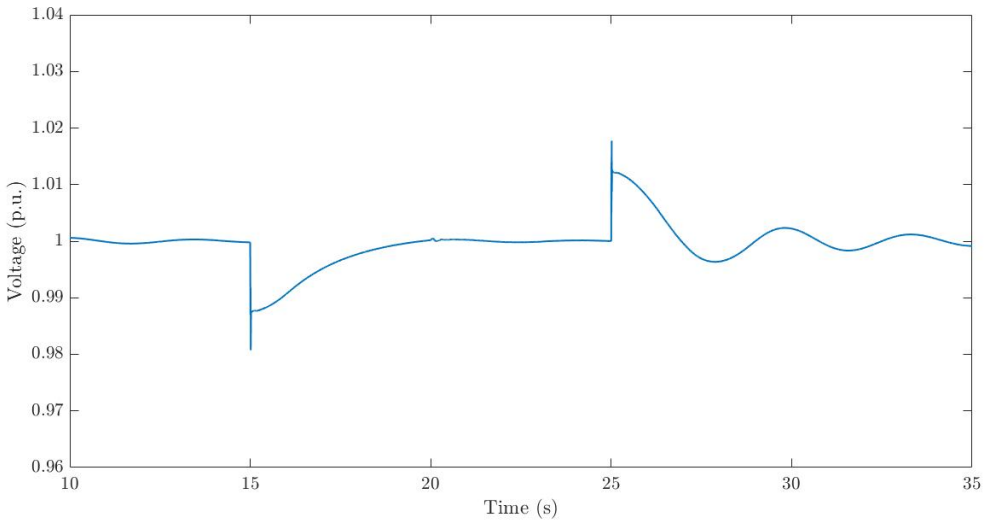

Figure 5.4: Voltage at PCC

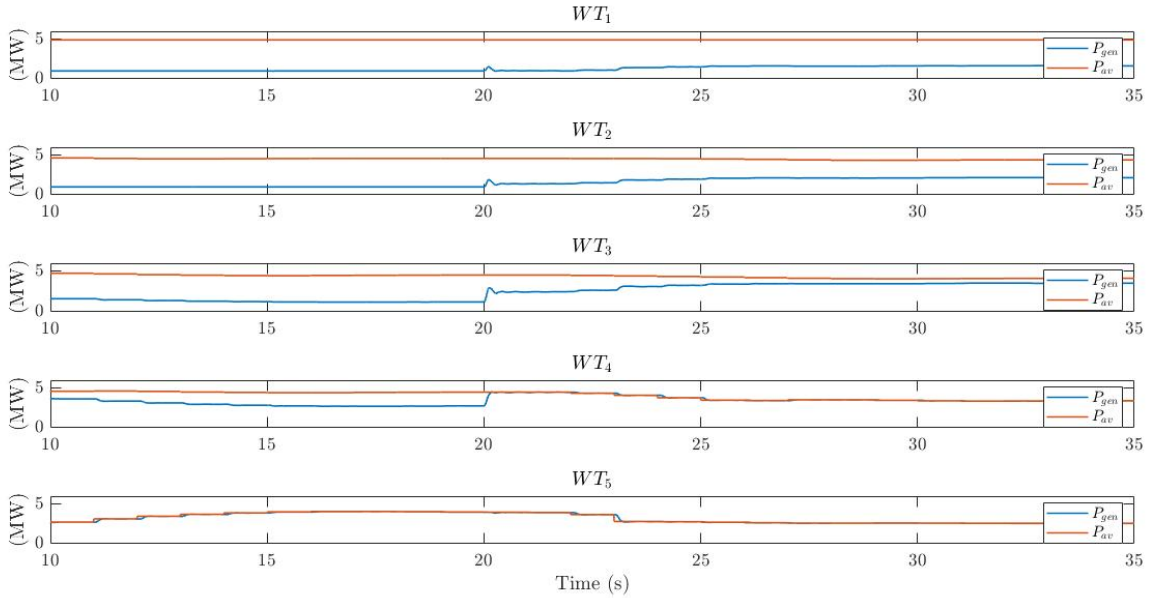

Figure 5.6: Active power contribution in a row of wind turbines

It can be noticed, Figure 5.5, that the reactive power contribution of the more up-stream wind turbines is slightly higher than the one of the downstream ones (WT_4 and WT_5). This is due to the fact that, as the wind farm is operating under a backward distribution control approach, the reactive capability of the downstream turbines is lower than the upstream ones, as their active power generation set-point is higher. The results presented only show a single row of the wind farm, however, as the wind direction considerate is 0^o, the wake effect and the power available at each turbine in the other rows are symmetrical to the ones of the first row. Hence, the individual power contribution set by the controller for the second and third row of wind turbines is equal to the first one.

In Figure 5.6 the distribution of the active power contribution of the first row of the wind farm is illustrated. As previously explained, having the same wake effect in the three rows, in the other two rows the active power distribution can be considered equal. It can be seen that, according with the objective of having a backward distribution of the active power, the most downstream turbines have a higher power set point; the last turbine operates at its maximum available power, permitting the others to have a significant amount of power reserve. At 20 s, when the step in power demand is applied and the wind farm has to inject 10 MW more of active power, it can be noticed that WT_4 and WT_3 start operating close to their available power while the WT_1 and WT_2 still have a low power set-point.

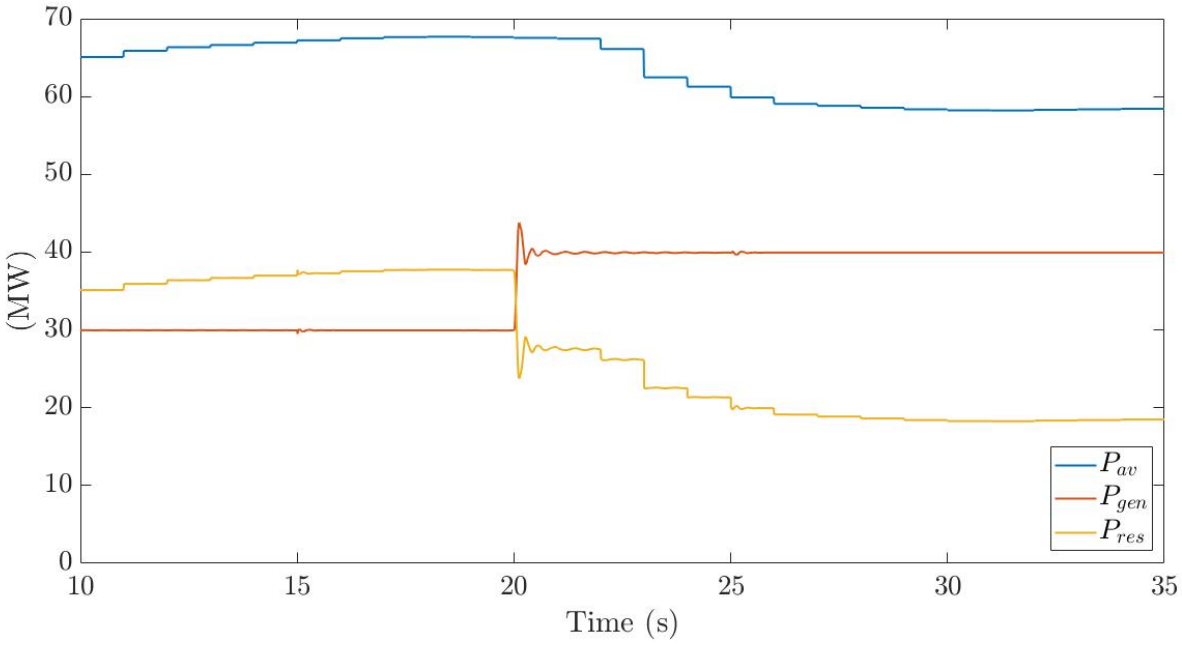

Figure 5.7: Total available, generated and reserve power of the wind farm

To conclude, Figure 5.7, shows how the tracking of the power demand is ensured by the wind farm, even applying a step at 20 s.

Chapter 6

Conclusions and further work

This master thesis has proposed two MPC strategies: one for maximizing the power reserve of a wind farm while tracking the power demand set by the TSOs and the second for regulating the voltage at the PCC while respecting the objectives mentioned in the first strategy.

In the first part of this thesis, based on the purpose of providing frequency support, a comparison was made between the conventional control strategies and the one proposed seeking to maximize the power reserve. The latter prioritizes the power contribution of the most downstream turbines and therefore minimizes the wake effect.

It was validated through several simulations with SimWindFarm toolbox, that the proposed approach has significant advantages especially when the wind turbines in the wake are close to each other and the WPPs work in important deloading operation mode. This approach could therefore augment the participation of wind farms in the frequency regulation market, providing benefits both for grid stability and in reducing the cost of wind generation.

In the second part, regarding the MPC formulation for the reactive power control, this study presents only some preliminary results. It was proven that the MPC controller is able to handle the different objectives of the optimization problem, tracking correctly the power demand, maintaining the voltage within this operation range and distributing the active power prioritizing the most downstream turbine. However, the sensitivity coefficient should be calculated following one of the validated approaches presented in literature in order to increase the performances of the controller. Once these results obtained, the tuning of the MPC should be performed again, to achieve better tracking performances and reduce the peaks and oscillations.

Left as further research is the validation of the performances of the control algorithm with high fidely wind farm models. Furthermore, an analysis of the impact of the proposed individual WTs power distribution on the mechanical loads and the lifetime of the turbines should be performed.

Finally, regarding the second part of the thesis, a study should be conducted on the effect of active power regulation on the PCC voltage, as it could be used for speed up the restoration of the voltage within its operational limits.

Appendix A: Environmental Impact

In order to face the challenges of our era and obtain a carbon neutral electricity grid mix, the development of renewable generation and especially wind power plants is crucial. However, the increase of renewable power production compromises the stability of the grid. To solve this issue, WPPs are required to provide ancillary services which usually involve a lower set-point of power production than the available one. As the development of a wind farm is capital intensive, in order to encourage investments in wind energy it is important to maximize the revenues from the power plant operation.
Hopefully, this research project can contribute to better understand how to optimize the operation of WPPs in order to enhance their participation in the ancillary service market. If wind farm are controlled and operated considering this goal, while improving the grid stability, the cost of wind energy can decrease and therefore boost the deployment of WPPs. This will positively affect the CO_2 emissions of the energy sector.

Appendix B: Budget

This section aims to present the costs associated with the development of this project. In the past seven months, the hours devoted to the project were 880. In the following table the tasks associated with the labour cost are presented:

Item	Quantity	Price	Total
Research hours	220 h	8 €/h	1760 €
Development hours	440 h	8 €/h	3520€
Writing hours	220 h	8 €/h	1760€
Total	880 h		7040 €

Table 6.1: Labour costs

The hardware used for simulations and the Matlab license were provided by university, CITCEA-UPC lab and IREC, and therefore are not directly included in the cost of this project.

Bibliography

[1] IEA. *Weo 2018*. 2018.

[2] Christine Lins et al. *10 YEARS OF RENEWABLE ENERGY PROGRESS*. Tech. rep. 2015.

[3] International Renewable Energy Agency. *Renewable capacity statistics 2018 Statistiques de capacité renouvelable 2018 Estadísticas de capacidad renovable 2018*. 2018, pp. 1–300.

[4] Ivan Komusanac, Daniel Fraile, and Guy Brindley. "Wind energy in Europe in 2018 - Trends and statistics". In: (2019), p. 32.

[5] Aloys Nghiem and Iván Pineda. "Wind energy in Europe: Scenarios for 2030". In: *Wind Europe* September (2017), p. 32.

[6] Jacob Aho et al. "A tutorial of wind turbine control for supporting grid frequency through active power control". In: *Proceedings of the American Control Conference* (2012), pp. 3120–3131.

[7] Ahmad Hemami. *Wind Turbine Technology*. 2012.

[8] Marcelo Gustavo and Pedro Enrique. "Modelling and Control Design of Pitch-Controlled Variable Speed Wind Turbines". In: *Wind Turbines* April 2011 (2012).

[9] Dirk Van Hertem, Oriol Gomis-Bellmunt, and Jun Liang. *HVDC Grids for Offshore and Supergrid of the Future*. 2016.

[10] Thomas Ackermann. *Wind power in power systems*. John Wiley & Sons, Ltd, 2005.

[11] James Carroll et al. "Availability, operation and maintenance costs of offshore wind turbines with different drive train configurations". In: *Wind Energy* 20.2 (2017), pp. 361–378.

[12] Fernando D. Bianchi, Hernan De Battista, and Ricardo J. Mantz. *Wind Turbine Control Systems*. 2007.

[13] Leon Freris. *Renewable energy in power systems*. Vol. 46. 08. 2013, pp. 46–4469–46–4469.

[14] S Boersma et al. "A Tutorial on Control-Oriented Modeling and Control of Wind Farms". In: (2017).

[15] N O Jensen. "A note on wind generator interaction". In: *Risø-M-2411 Risø National Laboratory Roskilde* (1983), pp. 1–16. eprint: arXiv:1011.1669v3.

[16] Sara Siniscalchi-Minna, Carlos Ocampo-Martinez, and Fernando D. Bianchi. "Partitioning approach for large wind farms: Active power control for optimizing power reserve". In: ().

[17] Sara Siniscalchi-Minna et al. "A wind farm control strategy for power reserve maximization". In: *Renewable Energy* 131 (2019), pp. 37–44.

[18] Jan Willem van Wingerden et al. "Active Power Control of Waked Wind Farms". In: *IFAC-PapersOnLine* 50.1 (2017), pp. 4484–4491.

[19] Paul Fleming et al. "Computational fluid dynamics simulation study of active power control in wind plants". In: *Proceedings of the American Control Conference* 2016-July (2016), pp. 1413–1420.

[20] Mehdi Vali et al. "Adjoint-based model predictive control of wind farms: Beyond the quasi steady-state power maximization". In: *IFAC-PapersOnLine* 50.1 (2017), pp. 4510–4515.

[21] *Online-measurement of the mains frequency*.

[22] E Ela et al. "Active Power Controls from Wind Power : Bridging the Gaps". In: January (2014).

[23] Oriol Gomis. *Grid support from renewable energy*. PowerPoint Presentation.

[24] B Kirby, M Milligan, and E Ela. "Providing Minute-to-Minute Regulation from Wind Plants". In: *Providing Minute-to-Minute Regulation from Wind Plants* October (2010), p. 11.

[25] Anca D. Hansen et al. "Centralised power control of wind farm with doubly fed induction generators". In: *Renewable Energy* 31.7 (2006), pp. 935–951.

[26] Ahmad Shabir Ahmadyar and Gregor Verbic. "Control strategy for optimal participation of wind farms in primary frequency control". In: *2015 IEEE Eindhoven PowerTech, PowerTech 2015* i (2015).

[27] Carl R. Shapiro et al. "Model-based receding horizon control of wind farms for secondary frequency regulation". In: *Wind Energy* 20.7 (2017), pp. 1261–1275.

[28] Sara Siniscalchi-Minna, Fernando D. Bianchi, and Carlos Ocampo-Martinez. "Predictive control of wind farms based on lexicographic minimizers for power reserve maximization". In: *Proceedings of the American Control Conference* 2018-June (2018), pp. 701–706.

[29] F. González-Longatt, P. P. Wall, and V. Terzija. "Wake effect in wind farm performance: Steady-state and dynamic behavior". In: *Renewable Energy* 39.1 (2012), pp. 329–338.

[30] J.M. Maciejowski. *Predictive Control with Constraints*. 2002.

[31] Julian Barreiro Gomez. "THE ROLE OF POPULATION GAMES IN THE DESIGN OF OPTIMIZATION-BASED CONTROLLERS : A LARGE-SCALE INSIGHT". PhD thesis. Universitat Politecnica de Catalunya, Universidad de los Antes.

[32] Jacob D. Grunnet et al. "Aeolus toolbox for dynamics wind farm model, simulation and control". In: *European Wind Energy Conference and Exhibition 2010, EWEC 2010* 4 (2010), pp. 3119–3129.

[33] Johan Löfberg. "YALMIP: A toolbox for modeling and optimization in MATLAB". In: *Proceedings of the IEEE International Symposium on Computer-Aided Control System Design* (2004), pp. 284–289.

[34] Haoran Zhao et al. "Coordinated voltage control of a wind farm based on model predictive control". In: *IEEE Transactions on Sustainable Energy* 7.4 (2016), pp. 1440–1451.

[35] Yifei Guo et al. "Enhanced voltage control of VSC-HVDC-connected offshore wind farms based on model predictive control". In: *IEEE Transactions on Sustainable Energy* 9.1 (2018), pp. 474–487.

[36] H. Zhao et al. "Combined Active and Reactive Power Control of Wind Farms Based on Model Predictive Control". In: *International Journal of Electrical Power and Energy Systems* 104.3 (2019), pp. 78–88.

[37] Nicholas W Miller, William W Price, and Juan J Sanchez-Gasca. "GE-Power Systems Energy Consulting Dynamic Modeling of GE 1.5 and 3.6 Wind Turbine-Generators GE Power Systems". In: (2003).

[38] Dheerah Kumar Khatod, Vinay Pant, and Jaydev Sharma. "A novel approach for sensitivity calculations in the radial distribution system". In: *IEEE Transactions on Power Delivery* 21.4 (2006), pp. 2048–2057.

[39] Konstantina Christakou et al. "Efficient computation of sensitivity coefficients of node voltages and line currents in unbalanced radial electrical distribution networks". In: *IEEE Transactions on Smart Grid* 4.2 (2013), pp. 741–750.